tions at the highest radiation dose. We speculate that NNK treatments plus radiation at the highest dose may induce p53-dependent apoptosis, which eliminates the cells bearing radiation-induced DSBs in DNA [29]. The involvement of p53 in the maintenance of genome stability is associated with several pathways such as cell cycle arrest, apoptosis and DNA repair. Low levels of DNA damage appear to enhance p53-dependent DNA repair while high levels induce apoptosis [30]. We envisage that NNK treatments plus radiation at the highest dose introduce genotoxic damage to the cells, the levels of which are enough to trigger the apoptosis. Zhou et al. [31] examined the combined effects of NNK and α-particle irradiation with human–hamster hybrid cultured cells and concluded that the induction of chromosome deletions were additive when the NNK dose was low but a suppressive effect was observed at a higher NNK concentration. In vivo studies also suggest that exposure to high levels of cigarette smoke decrease the risk of lung cancer induced by radon in dogs [32]. However, a multiplicative effect of smoking and radon is observed in rats [33]. In humans, the definitive interaction models have not been established between smoking and radiation exposure [24,25]. Thus, further work is needed to clearly establish the interactive genotoxic mechanisms between radiation and cigarette smoking in vivo.

NNK, a tobacco-specific nitrosamine, is metabolically activated by α-hydroxylation of the methyl and methylene groups [34]. Methylene hydroxylation leads to DNA methylation while methyl hydroxylation leads to pyridyloxobutylated DNA [35]. DNA methylation occurs at N7 and O^6 of guanine and O^4 and O^2 of thymine. It is suggested that O^6-methylguanine (O^6-mG) and pyridyloxobutylated DNA are responsible for G:C to A:T and G:C to T:A mutations, respectively, which activate Ki-*ras* oncogene in the mouse lung tumors induced by NNK [6]. In the present study, G:C to A:T and G:C to T:A mutations were induced by NNK treatments significantly (Table 1). Tiano et al. [36] examined the genotoxicity of NNK in AS52 hamster cells expressing human CYP2A6 and analyzed the induced mutations with the *gpt* gene as a reporter gene for mutations. Because of the lack of O^6-mG methyltransferase in the cell line, about 80% of mutations were G:C to A:T transitions. Interestingly, most of the G:C to A:T transition hotspots occur at the second G of the GGT sequence motif, which is the motif of codon 12 in the Ki-*ras* oncogene [37]. When we define the hotspot as the site where more than four G:C to A:T mutations were identified, we identified 18 hotspots in the *gpt* gene among 155 G:C to A:T mutants recovered from NNK-treated mice. They are nucleotide 27, 64, 86, 87, 92, 107, 110, 113, 115, 116, 128, 274, 281, 287, 402, 409, 417 and 418 when A of ATG of the start codon of the *gpt* gene is set as nucleotide 1. Tiano et al. [36] identified four hotspots of the second G of GGT in nucleotide 23, 116, 128 and 281 in the *gpt* gene, three of which are included in the hotspots identified by us. However, we identified other hotspots such as the second G of GGA at nucleotide 87, 274, 402 and 418, the second G of GGG at nucleotide 27, 64, 92 and 417 and the second G of GGC at nucleotide 113. Thus, we conclude that NNK preferentially induces G:C to A:T mutations at the second G of GGX where X represents any of A, T, G and C. In addition to G:C to A:T and G:C to T:A mutations, we observed an increase in the MFs of A:T to T:A and A:T to C:G in the NNK treated mice (Table 1). Substantial increases in the MFs of A:T to T:A and A:T to C:G are also reported by Hashimoto et al. [38], who examined the genotoxicity of NNK with *lacZ* transgenic mice (Muta^{TM} Mouse). Since reporter genes for mutations, such as *gpt*, *cII* or *lacZ*, are not expressed in vivo and are not imposed by any selection bias, they can reflect any genotoxic events occurring in the genomic DNA. In contrast, oncogenes such as the *ras* gene can only detect mutations that can activate the oncogenic activity of the gene products. Thus, we assume that NNK induces modifications in DNA such as O^4-methyl or O^2-methyl thymine in the lung, which may account for the induction of A:T to C:G and A:T to T:A mutations, respectively [8]. Although the toxicological significance of these mutations is currently unknown, these mutations may contribute to the carcinogenicity of cigarette smoke as well.

γ-Irradiation at dose rate of 1.0 and 1.5 mGy/h clearly enhanced the MFs of large deletions when no NNK treatments were combined (Fig. 3A). The total estimated doses were 0.68 and 1.02 Gy, which may be the lowest radiation doses that gave positive results in transgenic mice mutation assays [16]. In contrast, we could detect no significant increase in the MF of large deletions induced by NNK treatments (Table 2 and Fig. 3A and B). Thus, we suggest that NNK induces mostly base substitutions but not deletions in vivo. Interestingly, NNK treatments induce deletions in cultured mammalian cells. Tiano et al. [36] report that about 20% of mutations induced by NNK treatments are deletions in AS52 hamster cells expressing human CYP2A6. Zhou et al. [31] report that about 80% of NNK-induced mutations are large deletions in the human–hamster hybrid (A_L) cell assay. We speculate that NNK may have a potential to induce both base substitutions and large deletions in vitro but the latter can be eliminated in vivo by the p53-dependent mechanism. Chinese hamster cell lines such as CHO and V79 harbor missense mutation in the *p53*

gene [39,40]. Large deletions might have been detected in the cultured cells because of inefficient p53 functions.

In summary, we have examined the combined genotoxicity of γ-irradiation and NNK treatments in the lung of *gpt* delta mice. Although radiation did not modulate the NNK-induced base substitutions, NNK treatments suppressed the induction of large deletions in size more than 1 kb induced by the irradiation. NNK treatments might induce an adaptive response, which eliminates the cells bearing radiation-induced DSBs in DNA. This finding may be helpful in understanding the molecular mechanisms of genotoxicity as a result of interactions of more than one genotoxic agents in vivo.

Acknowledgements

Part of this study was financially supported by the Budget for Nuclear Research of the Ministry of Education, Culture, Sports, Science and Technology, based on the screening and counseling by the Atomic Energy Commission, and the Tutikawa Memorial Fund for Study in Mammalian Mutagenicity.

References

[1] R. Doll, R. Peto, The causes of cancer: quantitative estimates of avoidable risks of cancer in the United States today, J. Natl. Cancer Inst. 66 (1981) 1191–1308.
[2] Tobacco smoke and involuntary smoking, IARC Monogr Eval. Carcinog. Risk Chem. Hum., vol. 83, International Agency for Research on Cancer, Lyon, France, 2002.
[3] S.S. Hecht, Biochemistry, biology, and carcinogenicity of tobacco-specific *N*-nitrosamines, Chem. Res. Toxicol. 11 (1998) 559–603.
[4] S.S. Hecht, Tobacco carcinogens, their biomarkers and tobacco-induced cancer, Nat. Rev. Cancer 3 (2003) 733–744.
[5] International Agency for Research on Cancer Press Release, vol. 154, International Agency for Research on Cancer, Lyon, France, 2004.
[6] Z.A. Ronai, S. Gradia, L.A. Peterson, S.S. Hecht, G to A transitions and G toT transversions in codon 12 of the Ki-*ras* oncogene isolated from mouse lung tumors induced by 4-(methylnitrosamino)-1-(3-pyridyl)-1-butanone (NNK) and related DNA methylating and pyridyloxobutylating agents, Carcinogenesis 14 (1993) 2419–2422.
[7] R. Guza, M. Rajesh, Q. Fang, A.E. Pegg, N. Tretyakova, Kinetics of O^6-methyl-2′-deoxyguanosine repair by O^6-alkylguanine DNA alkyltransferase within *K-ras* gene-derived DNA sequences, Chem. Res. Toxicol. 19 (2006) 531–538.
[8] E.C. Friedberg, G.C. Walker, W. Siede, R.D. Wood, R.A. Schultz, T. Ellenberger, DNA Repair and Mutagenesis, 2nd ed., ASM Press, Washington, DC, 2006, pp. 1–1118.
[9] United Nations Scientific Committee on the Effects of Atomic Radiation, Sources, Effects and Risks of Ionising Radiation, 1988 Report to the General Assembly with Annexes, United Nations Press, New York, 1989.
[10] J.H. Lubin, K. Steindorf, Cigarette use and the estimation of lung cancer attributable to radon in the United States, Radiat. Res. 141 (1995) 79–85.
[11] H.P. Leenhouts, M.J. Brugmans, Calculation of the 1995 lung cancer incidence in The Netherlands and Sweden caused by smoking and radon: risk implications for radon, Radiat. Environ. Biophys. 40 (2001) 11–21.
[12] United Nations Scientific Committee on the Effects of Atomic Radiation, Combined Effects of Radiation and Other Agents, Report to the General Assembly, United Nations Press, New York, 1998.
[13] M.S. Sasaki, Y. Ejima, A. Tachibana, T. Yamada, K. Ishizaki, T. Shimizu, T. Nomura, DNA damage response pathway in radioadaptive response, Mutat. Res. 504 (2002) 101–118.
[14] T. Lindahl, B. Sedgwick, M. Sekiguchi, Y. Nakabeppu, Regulation and expression of the adaptive response to alkylating agents, Annu. Rev. Biochem. 57 (1988) 133–157.
[15] N.G. Oliveira, M. Neves, A.S. Rodrigues, G.O. Monteiro, T. Chaveca, J. Rueff, Assessment of the adaptive response induced by quercetin using the MNCB peripheral blood human lymphocytes assay, Mutagenesis 15 (2000) 77–83.
[16] T. Nohmi, K.I. Masumura, *gpt* Delta transgenic mouse: a novel approach for molecular dissection of deletion mutations in vivo, Adv. Biophys. 38 (2004) 97–121.
[17] T. Nohmi, T. Suzuki, K. Masumura, Recent advances in the protocols of transgenic mouse mutation assays, Mutat. Res. 455 (2000) 191–215.
[18] M. Miyazaki, H. Yamazaki, H. Takeuchi, K. Saoo, M. Yokohira, K. Masumura, T. Nohmi, Y. Funae, K. Imaida, T. Kamataki, Mechanisms of chemopreventive effects of 8-methoxypsoralen against 4-(methylnitrosamino)-1-(3-pyridyl)-1-butanone-induced mouse lung adenomas, Carcinogenesis 26 (2005) 1947–1955.
[19] T. Nohmi, M. Suzuki, K. Masumura, M. Yamada, K. Matsui, O. Ueda, H. Suzuki, M. Katoh, H. Ikeda, T. Sofuni, Spi$^-$ selection: an efficient method to detect gamma-ray-induced deletions in transgenic mice, Environ. Mol. Mutagen. 34 (1999) 9–15.
[20] K. Masumura, K. Kuniya, T. Kurobe, M. Fukuoka, F. Yatagai, T. Nohmi, Heavy-ion-induced mutations in the *gpt* delta transgenic mouse: comparison of mutation spectra induced by heavy-ion, X-ray, and gamma-ray radiation, Environ. Mol. Mutagen. 40 (2002) 207–215.
[21] T. Nohmi, K. Masumura, Molecular nature of intrachromosomal deletions and base substitutions induced by environmental mutagens, Environ. Mol. Mutagen. 45 (2005) 150–161.
[22] M. Horiguchi, K.I. Masumura, H. Ikehata, T. Ono, Y. Kanke, T. Nohmi, Molecular nature of ultraviolet B light-induced deletions in the murine epidermis, Cancer Res. 61 (2001) 3913–3918.
[23] W. Zhang, C. Wang, D. Chen, M. Minamihisamatsu, H. Morishima, Y. Yuan, L. Wei, T. Sugahara, I. Hayata, Effect of smoking on chromosomes compared with that of radiation in the residents of a high-background radiation area in China, J. Radiat. Res. (Tokyo) 45 (2004) 441–446.
[24] Z.B. Tokarskaya, B.R. Scott, G.V. Zhuntova, N.D. Okladnikova, Z.D. Belyaeva, V.F. Khokhryakov, H. Schollnberger, E.K. Vasilenko, Interaction of radiation and smoking in lung cancer induction among workers at the Mayak nuclear enterprise, Health Phys. 83 (2002) 833–846.
[25] V.E. Archer, Enhancement of lung cancer by cigarette smoking in uranium and other miners, Carcinog. Compr. Surv. 8 (1985) 23–37.

[26] K. Sakai, Y. Hoshi, T. Nomura, T. Oda, T. Iwasaki, K. Fujita, T. Yamada, H. Tanooka, Suppression of carcinogenic processes in mice by chronic low dose rate gamma-irradiation, Int. J. Low Radiat. 1 (2003) 142–146.
[27] S. Wolff, Failla memorial lecture. Is radiation all bad? The search for adaptation, Radiat. Res. 131 (1992) 117–123.
[28] J.D. Tucker, K.J. Sorensen, C.S. Chu, D.O. Nelson, M.J. Ramsey, C. Urlando, J.A. Heddle, The accumulation of chromosome aberrations and *Dlb-1* mutations in mice with highly fractionated exposure to gamma radiation, Mutat. Res. 400 (1998) 321–335.
[29] C.E. Canman, M.B. Kastan, Role of p53 in apoptosis, Adv. Pharm. 41 (1997) 429–460.
[30] H. Offer, N. Erez, I. Zurer, X. Tang, M. Milyavsky, N. Goldfinger, V. Rotter, The onset of p53-dependent DNA repair or apoptosis is determined by the level of accumulated damaged DNA, Carcinogenesis 23 (2002) 1025–1032.
[31] H. Zhou, L.X. Zhu, K. Li, T.K. Hei, Radon, tobacco-specific nitrosamine and mutagenesis in mammalian cells, Mutat. Res. 430 (1999) 145–153.
[32] F.T. Cross, R.F. Palmer, R.E. Filipy, G.E. Dagle, B.O. Stuart, Carcinogenic effects of radon daughters, uranium ore dust and cigarette smoke in beagle dogs, Health Phys. 42 (1982) 33–52.
[33] F.T. Cross, Radioactivity in cigarette smoke issue, Health Phys. 46 (1984) 205–208.
[34] S.S. Hecht, D. Hoffmann, Tobacco-specific nitrosamines, an important group of carcinogens in tobacco and tobacco smoke, Carcinogenesis 9 (1988) 875–884.
[35] Y. Lao, P.W. Villalta, S.J. Sturla, M. Wang, S.S. Hecht, Quantitation of pyridyloxobutyl DNA adducts of tobacco-specific nitrosamines in rat tissue DNA by high-performance liquid chromatography-electrospray ionization-tandem mass spectrometry, Chem. Res. Toxicol. 19 (2006) 674–682.
[36] H.F. Tiano, R.L. Wang, M. Hosokawa, C. Crespi, K.R. Tindall, R. Langenbach, Human CYP2A6 activation of 4-(methylnitrosamino)-1-(3-pyridyl)-1-butanone (NNK): mutational specificity in the *gpt* gene of AS52 cells, Carcinogenesis 15 (1994) 2859–2866.
[37] L.A. Peterson, S.S. Hecht, O^6-Methylguanine is a critical determinant of 4-(methylnitrosamino)-1-(3-pyridyl)-1-butanone tumorigenesis in A/J mouse lung, Cancer Res. 51 (1991) 5557–5564.
[38] K. Hashimoto, K. Ohsawa, M. Kimura, Mutations induced by 4-(methylnitrosamino)-1-(3-pyridyl)-1-butanone (NNK) in the *lacZ* and *cII* genes of Muta Mouse, Mutat. Res. 560 (2004) 119–131.
[39] H. Lee, J.M. Larner, J.L. Hamlin, Cloning and characterization of Chinese hamster p53 cDNA, Gene 184 (1997) 177–183.
[40] W. Chaung, L.J. Mi, R.J. Boorstein, The p53 status of Chinese hamster V79 cells frequently used for studies on DNA damage and DNA repair, Nucl. Acids Res. 25 (1997) 992–994.

Arch Toxicol (2007) 81:63–69
DOI 10.1007/s00204-006-0126-9

GENOTOXICITY AND CARCINOGENICITY

Lack of in vivo mutagenicity and oxidative DNA damage by flumequine in the livers of *gpt* delta mice

Yuichi Kuroiwa · Takashi Umemura · Akiyoshi Nishikawa · Keita Kanki · Yuji Ishii · Yukio Kodama · Ken-ichi Masumura · Takehiko Nohmi · Masao Hirose

Received: 3 March 2006 / Accepted: 1 June 2006 / Published online: 27 June 2006

Abstract Flumequine (FLU), an anti-bacterial quinolone agent, has been recognized as a non-genotoxic carcinogen for the mouse liver, but recent reports have suggested that some genotoxic mechanism involving oxidative DNA damage may be responsible for its hepatocarcinogenesis. In the present study, we investigated this possibility in the mouse liver using male and female B6C3F1 *gpt* delta mice fed diet containing 0.4% FLU, a carcinogenic dose, for 13 weeks. Measurements of 8-hydroxydeoxyguanosine levels in liver DNA, and *gpt* point and deletion mutations revealed no significant increases in any of these parameters in either sex. Histopathologically, centrilobular swelling of hepatocytes with vacuolation was apparent, however, together with significant increase in bromodeoxyuridine-labeling indices in the treated males and females. These results suggest that genotoxicity, including oxidative DNA damage, is not involved in mouse hepatocarcinogenesis by FLU, which might rather solely exert tumor-promoting effects in the liver.

Y. Kuroiwa · T. Umemura (✉) · A. Nishikawa · K. Kanki · Y. Ishii · M. Hirose
Division of Pathology, National Institute of Health Sciences, 1-18-1 Kamiyoga, Setagaya-ku, Tokyo 158-8501, Japan
e-mail: umemura@nihs.go.jp

Y. Kodama
Division of Toxicology, National Institute of Health Sciences, 1-18-1 Kamiyoga, Setagaya-ku, Tokyo 158-8501, Japan

K. Masumura · T. Nohmi
Division of Genetics and Mutagenesis, National Institute of Health Sciences, 1-18-1 Kamiyoga, Setagaya-ku, Tokyo 158-8501, Japan

Keywords Flumequine · In vivo mutagenicity · Oxidative DNA damage · Cell proliferation · *gpt* delta mouse

Introduction

Flumequine (FLU) is a fluoroquinolone compound with anti-microbial activity against gram-negative organisms used in the treatment of enteric infections in domestic animals (Greenwood 1998), which has also limited application in humans for the treatment of urinary tract infections (JECFA 2004). Flumequine and its metabolites are suspected to persist in the edible tissues of domestic animals and fish (Choma et al. 1999). Toxicity and carcinogenicity studies of FLU have already been performed using rats and mice, and FLU-induced hepatocellular tumors in an 18-month carcinogenicity study in CD-1 mice (JECFA 1998). However, negative results were obtained in an in vivo chromosome aberration test, a reverse mutation test in bacteria and gene mutation tests in mammalian cells (JECFA 1998). On the basis of these data, the Food and Agriculture Organization (FAO)/World Health Organization (WHO) Joint Expert Committee on Food Additives (JECFA) concluded that FLU is a non-genotoxic hepatocarcinogen, and that hepatocellular necrosis-regeneration cycles due to hepatotoxicity are mechanistically relevant to its induction of liver tumors in mice (JECFA 1998).

Previously, Yoshida et al. (1999) reported that the administration of FLU in the diet at a concentration of 4,000 ppm for 30 weeks induced basophilic liver cell foci in CD-1 mice and also increased the number of 8-hydroxydeoxyguanosine (8-OHdG) positive hepato-

cytes immunohistochemically. In addition, heterozygous *p53*-deficient CBA mice, a strain sensitive to genotoxic carcinogens, receiving 4,000 ppm FLU for 26 weeks developed basophilic liver foci (Takizawa et al. 2001). Positive results of in vivo comet assays in ddY mice, and increases of the number of hepatocellular foci in C3H mice using a two-stage liver carcinogenesis model have also been reported (Kashida et al. 2002), strongly pointing to a necessity for determination of whether FLU has initiating potential for mouse liver. Based on the results, JECFA temporarily withdrew the acceptable daily intake values (ADI), but this was shortly re-established at 0–30 mg/kg bw based on negative results for unscheduled DNA synthesis with FLU in rat liver cells in vivo (JECFA 2003, 2004). Thus, since conclusive evidence regarding the mode of action of FLU has yet to be provided, clarification of its in vivo mutagenicity is required for accurate assessment of hazard risk for humans.

Rodents transfected with *gpt* as a reporter gene are useful tools for estimating in vivo genotoxicity and carcinogenic risk of environmental chemicals (Gorelich et al. 1996; Nohmi et al. 2000; Nishikawa et al. 2001). In this transgenic mouse mutation assay, the reporter gene is integrated into mouse chromosome as part of λ shuttle vectors, which are easily recovered as phage particles from mouse genomic DNA by in vitro packaging reactions. Transgenic mice carrying the λ vector are treated with a test compound, and the mutant phages are infected to specific *E. coli* host cells and selected. An advantage of this *gpt* delta mouse model is to be able to detect two distinct types of mutations: point mutations can be positively identified by 6-thioguanine (6-TG) selection and deletions with sizes of more than 1 K base pairs by Spi^- selection (Nohmi et al. 2000). In the present study, we therefore performed in vivo mutation assays of FLU using B6C3F1 *gpt* delta mice, along with measurement of 8-OHdG formation in liver DNA and hepatocyte bromodeoxyuridine-labeling indices (BrdU-LIs).

Materials and methods

Chemicals

Flumequine, a white crystallized powder (purity 99.3%), was kindly provided by Kyowa Hakko Kogyo Co., Ltd. (Tokyo, Japan). Alkaline phosphatase and BrdU were obtained from Sigma Chemical Co. (St. Louis, MO, USA) and nuclease P1 from Yamasa Co. (Chiba, Japan).

Animals and treatments

The protocol for this study was approved by the Animal Care and Utilization Committee of the National Institute of Health Sciences. Male and female B6C3F1 *gpt* delta mice carrying 80 tandem copies of the transgene lambda EG10 in haploid genome were raised from mating between C57BL/6 *gpt* delta and non-transgenic C3H/He mice, a strain of mice with high sensitivity to hepatocarcinogens (Japan SLC, Inc. Shizuoka, Japan). Twenty male and 20 female B6C3F1 *gpt* delta mice were each randomized by weight into two groups. They were housed in a room with a barrier system, and maintained under the following constant conditions: temperature of 23 ± 2°C, relative humidity of 55 ± 5%, ventilation frequency of 18 times/h, and a 12 h light–dark cycle, with free access to CRF-1 basal diet (Oriental Yeast Co., Ltd., Tokyo, Japan) and tap water.

Starting at 8 weeks of age the mice were fed diet containing 0.4% FLU or maintained as non-treatment controls for 13 weeks. At the end of the experiment, five males and females from each group were sacrificed and a part of left lateral lobe of the liver was preserved at –80°C for subsequent mutation assays and 8-OHdG measurement. The rest of the lobes were fixed in 10% buffered formalin solution and routinely processed to paraffin blocks for histopathological examination as well as immunohistochemistry. Hematoxylin and eosin (H–E)-stained tissue preparations cut from the blocks were examined by light microscopy. At autopsy, the body and liver weights were measured.

Quantification of hepatocyte proliferation

In order to examine the proliferative activity of hepatocytes, the remaining five animals from each group not used for other analyses were given BrdU (100 mg/kg) by i.p. injection once a day for the final 2 days and once on the day of termination at 2 h before being euthanatized at autopsy. For immunohistochemical staining of BrdU, after first denaturing DNA with 4*N* HCl, tissue sections were treated sequentially with normal horse serum, monoclonal mouse anti-BrdU (Becton, Dickinson & Co., Franklin Lakes, NJ, USA) (1:100), biotin-labeled horse anti-mouse IgG (1:400), and avidin–biotin–peroxidase complex (Vectastain ABC kit, Vector Laboratories, Inc., Burlingame, CA, USA). The site of peroxidase binding was demonstrated by incubation with 3,3′-diaminobenzidine tetrahydrochloride (Sigma-Aldrich Co.). The immunostained sections were lightly counterstained with hematoxylin for microscopic examination. At least

2,000 hepatocytes in each liver were counted and labeling indices (LIs) were calculated as the percentages of cells positive for BrdU incorporation.

Measurement of 8-OHdG in liver DNA

In order to prevent 8-OHdG formation as a byproduct during DNA isolation (Kasai 2002), liver DNA was extracted by a slight modification of the method of Nakae et al. (1995). Briefly, nuclear DNA was extracted with a commercially available DNA Extractor WB Kit (Wako Pure Chemical Industries, Ltd., Osaka, Japan) containing antioxidant NaI solution to dissolve cellular components. For further prevention of autooxidation in the cell lysis step, deferoxamine mesylate (Sigma Chemical Co.) was added to the lysis buffer (Helbock et al. 1998). The DNA was digested to deoxynucleotides with nuclease P1 and alkaline phosphatase and levels of 8-OHdG (8-OHdG/10^5 deoxyguanosine) were assessed by high-performance liquid chromatography (HPLC) with an electrochemical detection system (Coulochem II, ESA, Bedford, MA, USA).

In vivo mutation assays

6-TG and Spi$^-$ selection were performed as previously described (Nohmi et al. 2000). Briefly, genomic DNA was extracted from each liver, and lambda EG10 DNA (48 kb) was rescued as the lambda phage by in vitro packaging. For 6-TG selection, the packaged phage was incubated with *E. coli* YG6020, which expresses Cre recombinase, and converted to a plasmid carrying *gpt* and chloramphenicol acetyltransferase. Infected cells were mixed with molten soft agar and poured onto agar plates containing chloramphenicol and 6-TG. In order to determine the total number of rescued plasmids, 3,000-fold diluted phages were used to infect YG6020, and were poured on the plates containing chloramphenicol without 6-TG. The plates were incubated at 37°C for selection of 6-TG-resistant colonies. Positively selected colonies were counted on day 3 and collected on day 4. The mutant frequency was calculated by dividing the number of *gpt* mutants by the number of rescued phages.

For the Spi$^-$ selection, the packaged phage was incubated with *E. coli* XL-1 Blue MRA for survival titration and *E. coli* XL-1 Blue MRA P2 for mutant selection. Infected cells were mixed with molten lambda-trypticase soft agar and poured onto lambda-trypticase agar plates. Next day, plaques (Spi$^-$ candidates) were punched out with sterilized glass pipettes and the agar plugs were suspended in SM buffer. In order to confirm the Spi$^-$ phenotype of candidates, the suspensions were spotted on three types of plates on which XL-1 Blue MRA, XL-1 Blue MRA P2, or WL95 P2 strains were spread with soft agar. Real Spi$^-$ mutants, which made clear plaques on every plate, were counted.

Statistical evaluation

For statistical analysis, the Student's *t* test was used to compare liver and body weights, as well as quantitative data for BrdU-LIs, 8-OHdG levels and MFs, between groups.

Results

Body and liver weights and FLU intake

Data for final body and organ weights and intake of FLU are shown in Table 1. The final body weights were significantly ($P < 0.01$) decreased in FLU-treated males and females. Daily food consumption was also decreased in the FLU-treated animals, particularly females, as compared to the control group value. Daily FLU intake calculated from the consumption values were 590 and 763 mg/kg/day in males and females, respectively (Table 1). The doses used in a previous carcinogenicity study by gavage were 400 and 800 mg/kg/day, both of which were carcinogenic in mice (JECFA 2004). Liver/body weight ratios were significantly ($P < 0.01$) increased in the FLU-treated males and females.

Histopathology and immunohistochemical analysis of BrdU

Histopathologically, swelling of centrilobular hepatocytes with vacuolation was observed in FLU-treated males (Fig. 1b) and females. Slight infiltration of lymphocytes and neutrophils was also observed, although distinct hepatocellular necrosis was not found. There were no distinct sex differences in the degree of lesion development. The number of BrdU-positive liver cells (Fig. 1c, d) was increased in the FLU-treated group (Fig. 2), mostly appearing in the mid-zone of normal-looking cells adjacent to the damaged cells. The BrdU-LI in males given FLU was significantly ($P < 0.05$) higher than that in females (Fig. 2).

8-OHdG level in liver DNA

The data for 8-OHdG levels in the livers of FLU-treated males and females are shown in Fig. 3. No

Table 1 Body and liver weights, and food and flumequine intake data

Treatment	Number of mice	Body weight (g)[a]	Liver/body weight ratio (%)[a]	Food consumption (g/mouse/day)	Flumequine intake	
					Total (mg/mouse)	Daily (mg/kg/day)
Males						
Control	10	36.3 ± 1.0	4.56 ± 0.62	5.4	–	–
0.4% Flumequine	10	31.4 ± 1.5*	5.31 ± 0.24*	4.2	1,517	590
Females						
Control	10	25.7 ± 1.9	4.28 ± 0.25	7.0	–	–
0.4% Flumequine	10	23.3 ± 0.8*	5.42 ± 0.37*	4.4	1,610	763

[a]Data are mean ± SD values

*$P < 0.01$ (vs. control)

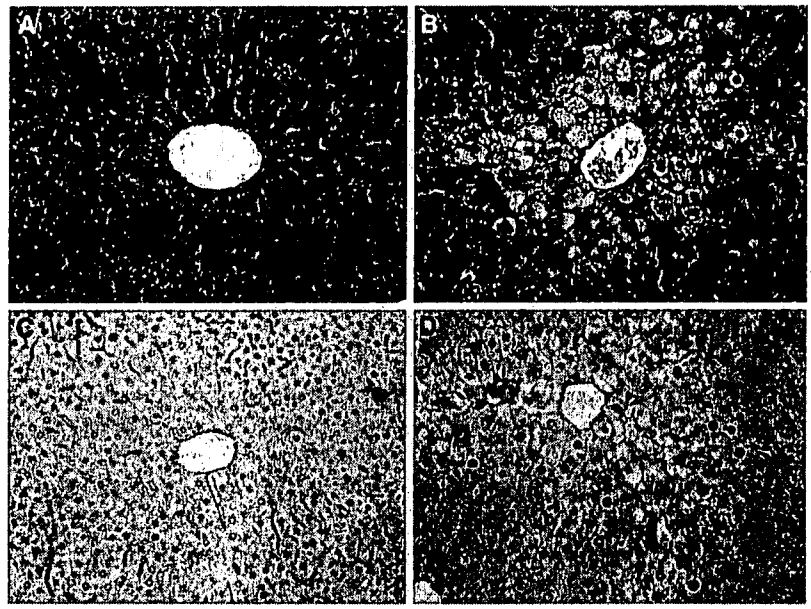

Fig. 1 Photomicrographs of livers of male gpt delta mice treated with basal diet (**a**, **c**) and 0.4% flumequine for 13 weeks (**b**, **d**). Note no obvious alterations (**a**) and centrilobular hepatocytes swelling with vacuolation (**b**). H–E staining at ×360 original magnification. Note BrdU-positive hepatocytes were few (**c**) and remarkably seen adjacent to the damaged cells (**d**). BrdU immunohistochemical staining at ×360 original magnification

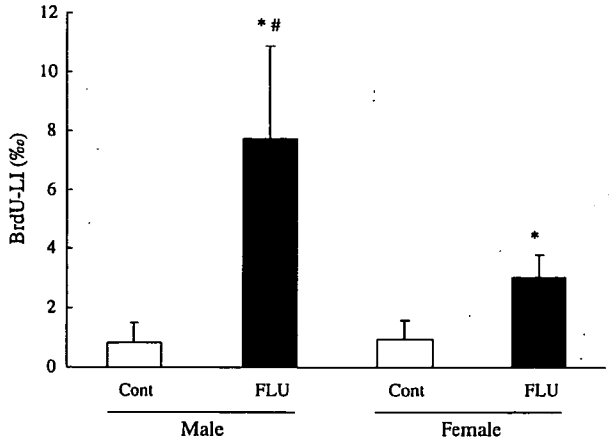

Fig. 2 BrdU-LIs for hepatocytes in male and female *gpt* delta mice fed 0.4% flumequine for 13 weeks. Values are mean ± SD of data for five mice. * Significant increase ($P < 0.05$) from the control group. # Significant difference ($P < 0.05$) between the sexes

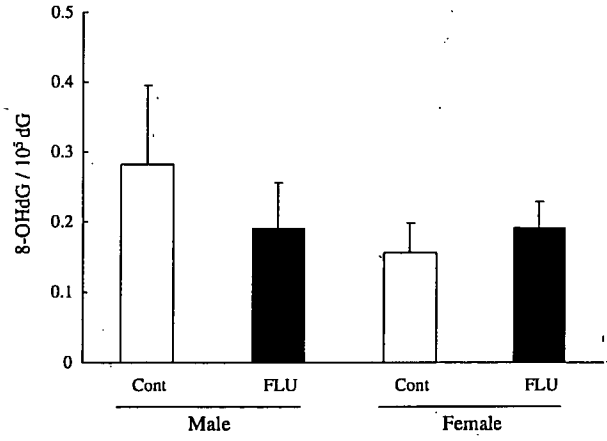

Fig. 3 8-OHdG levels in the livers of male and female *gpt* delta mice fed 0.4% flumequine for 13 weeks. Values are means ± SD of data for five mice. No significant differences were observed

Table 2 Guanine phosphoribosyltransferase *(gpt)* mutant frequencies (MFs) in the livers

Treatment	Number of mice	Total population	6-TG^r colonies	Total *gpt* mutants	MF ($\times 10^{-5}$)[a]
Male					
Control	5	3,378,000	27	22	0.80 ± 0.44
0.4% Flumequine	5	6,126,000	66	55	1.01 ± 0.52
Female					
Control	5	5,166,000	33	25	0.46 ± 0.28
0.4% Flumequine	5	6,864,000	63	43	0.65 ± 0.25

No significant difference was observed in MFs

[a]Data are mean ± SD values

significant effect of the FLU treatment was noted in either sex.

Mutation assays

Data for *gpt* MFs analyzed by 6-TG selection are summarized in Table 2. There were no significant increases of *gpt* MFs in the liver DNA of the FLU-treated males or females as compared to the non-treatment control values. Data for Spi$^-$ selection assessing deletion mutations are summarized in Table 3. Again, there was no significant variation in Spi$^-$ MFs values between FLU-treated and control mice.

Discussion

The present study did not provide support for the earlier finding from immunohistochemical analysis of increased 8-OHdG adducts in hepatocytes of mice given FLU (Yoshida et al. 1999). A marker widely used for oxidative damage to DNA (Shigenaga et al. 1991), 8-OHdG pairs with adenine as well as cytosine, generating GC-to-TA transversions upon replication by DNA polymerases (Cheng et al. 1992). Therefore, it has been postulated that this oxidized base is responsible for mutagenicity and carcinogenicity of many epigenetic carcinogens (Le Page et al. 1995; Nakae et al. 2002). In the present study, we quantitated 8-OHdG in the FLU-treated mouse livers by HPLC-ECD, but found no significant increase in either sex of treated mice. In addition to the fact that the present experimental conditions regarding animal strain and duration of exposure were different from these used previously (Yoshida et al. 1999), it is widely accepted that HPLC-ECD method is more precise and suitable for the detection of dose responses than immunohistochemistry (ESCODD 2000). There is a major body of evidence in favor of most sensitive detection of 8-OHdG elevation by HPLC-ECD in target organ DNA of animals exposed to hepatocarcinogens causing oxidative stress (Fiala et al. 1993; Umemura et al. 1996; Kasai 1997). Therefore, it is clear that FLU dose not cause oxidative DNA damage in the mouse liver at least under the present experimental conditions.

Table 3 Spi$^-$ MFs in the livers

Treatment	Number of mice	Total population	Total Spi$^-$ mutants	MF ($\times 10^{-5}$)[a]
Male				
Control	5	4,932,000	20	0.40 ± 0.14
0.4% Flumequine	5	5,350,500	20	0.38 ± 0.31
Female				
Control	5	7,587,000	25	0.33 ± 0.11
0.4% Flumequine	5	5,476,500	24	0.48 ± 0.36

No significant difference was observed in MFs

[a]Data are mean ± SD values

Similarly, in the present study, there were also no remarkable increases in *gpt* or Spi- mutation frequencies in the liver DNA of male or female *gpt* delta mice treated with FLU. We previously reported that many chemicals classified as genotoxic carcinogens increase mutation frequency with characteristic mutation spectra in target organ DNA of *gpt* delta mice (Nohmi and Masumura 2005; Kanki et al. 2005; Masumura at al. 2003). We also confirmed no increases of mutation frequency in the reporter gene in any organs of transgenic mice treated with non-genotoxic carcinogens or non-carcinogen, and in non-target organs treated with genotoxic carcinogens (Kanki et al. 2005; Nishikawa et al. 2001). Recently, we found that an increase in the mutation frequency with chemical exposure in a reported non-target organ was able to lead to tumor formation with the aid of an appropriate tumor-promoting regimen (Nishikawa et al. 2005). Thus, the data overall strongly suggest that the in vivo mutation assay using *gpt* delta mice is a reliable tool to predict the potential of a chemical for tumor-initiation. From the results of a comet assay for FLU, Kashida et al. (2002) suggested FLU cause DNA strand breaks in infant or regenerative livers of ddY mice, and sporadically in adult liver. However, the data were also in line with effects limited to cells with high mitotic activity. Although we should consider a possibility of other oxidative lesions than 8-OHdG occurring, the overall data

suggested that any lesions failed to exceed the thresholds for inducing their relevant genotoxicity. Accordingly, it can be said that FLU is not a tumor-initiating compound, genotoxicity including oxidative DNA damage not being involved in its hepatocarcinogenesis.

The present study revealed elevated cell proliferation in FLU-treatment in terms of BrdU incorporation, in agreement with a previous report of increase of proliferating cell nuclear antigen (PCNA)-positive cells in FLU-treated mice (Yoshida et al. 1999; Takizawa et al. 2001), and our data for liver weights. Together with the body weight suppression, these data imply hepatotoxicity of FLU (JECFA 1998; Yoshida et al. 1999). Focal necrosis of hepatocytes was observed in CD-1 mice at 400 and 800 mg/kg/day in an 18-month study earlier (JECFA 1998), although distinct hepatocellular necrosis was not found in the present study. The present finding that BrdU-LIs in FLU-treated males were significantly higher than in females corresponded to the previous report of a sex differentiation in FLU toxicity (JECFA 1998). Therefore, our data strongly support JECFA's conclusion that the induction of hepatocellular necrosis–regeneration cycles due to FLU hepatotoxicity is the relevant to 'promotion' of liver tumor development (JECFA 2004).

In conclusion, our data clearly demonstrate that FLU dose not cause either oxidative DNA damage or mutagenicity in the mouse liver when given even at a carcinogenic dose. Therefore, it is concluded that genotoxicity, including oxidative DNA damage, is not involved in mouse hepatocarcinogenesis by FLU and it can be classified as a mouse liver tumor promoter.

Acknowledgments We thank Ms. Machiko Maeda, Ayako Kaneko and Fukiko Takagi for their expert technical assistance in performing the animal experiments and processing histological materials. This work was supported in part by a Grant-in-Aid for research on safety of veterinary drug residues in food of animal origin from the Ministry of Health, Labour and Welfare, Japan.

References

Cheng KC, Cahill DS, Kasai H, Nishimura S, Loeb LA (1992) 8-Hydroxyguanine, an abundant form of oxidative DNA damage, causes G——T and A——C substitutions. J Biol Chem 267:166–172

Choma I, Grenda D, Malionwska I, Suprynowicz Z (1999) Determination of flumequine and doxycycline in milk by a simple thin-layer chromatographic method. J Chromatogr B Biomed Sci Appl 734:7–14

ESCODD (2000) Comparison of different methods of measuring 8-oxoguanine as a marker of oxidative DNA damage. ESCODD (European Standards Committee on Oxidative DNA Damage). Free Radic Res 32:333–341

Fiala ES, Nie G, Sodum R, Conaway CC, Sohn OS (1993) 2-Nitropropane-induced liver DNA and RNA base modifications: differences between Sprague-Dawley rats and New Zealand white rabbits. Cancer Lett 74:9–14

Gorelich NJ, Mirsalis JC (1996) A strategy for the application of transgenic rodent mutagenesis assays. Environ Mol Mutagen 28:434–442

Greenwood D (1998) Activity of flumequine against Escherichia coli: in vitro comparison with nalidixic and oxolinic acids. Antimicrob Agents Chemother 13:479–483

Helbock HJ, Beckman KB, Shigenaga MK, Walter PB, Woodall AA, Yeo HC, Ames BN (1998) DNA oxidation matters: the HPLC-electrochemical detection assay of 8-oxo-deoxyguanosine and 8-oxo-guanine. Proc Natl Acad Sci USA 95:288–293

JECFA (1998) Evaluation of certain veterinary drug residues in food. Forty-eighth report of the Joint FAO/WHO Expert Committee on food additives. World Health Organ Tech Rep Ser 879:35–43

JECFA (2003) Evaluation of certain veterinary drug residues in food. Sixtieth report of the Joint FAO/WHO Expert Committee on food additives. World Health Organ Tech Rep Ser 918:11–15

JECFA (2004) Evaluation of certain veterinary drug residues in food. Sixty-second report of the Joint FAO/WHO Expert Committee on food additives. World Health Organ Tech Rep Ser 925:18–19

Kanki K, Nishikawa A, Masumura K, Umemura T, Imazawa T, Kitamura Y, Nohmi T, Hirose M (2005) In vivo mutational analysis of liver DNA in gpt delta transgenic rats treated with the hepatocarcinogens N-nitrosopyrrolidine, 2-amino-3-methylimidazo[4,5-f]quinoline, and di(2-ethylhexyl)phthalate. Mol Carcinog 42:9–17

Kasai H (1997) Analysis of a form of oxidative DNA damage, 8-hydroxy-2'-deoxyguanosine, as a marker of cellular oxidative stress during carcinogenesis. Mutat Res 387:147–163

Kasai H (2002) Chemistry-based studies on oxidative DNA damage: formation, repair, and mutagenesis. Free Radic Biol Med 33:450–456

Kashida Y, Sasaki YF, Ohsawa K, Yokohama A, Watanabe T, Mitsumori K (2002) Mechanistic study on flumequine hepatocarcinogenecity focusing on DNA damage in mice. Toxicol Sci 69:317–321

Le Page F, Margot A, Grollman AP, Sarasin A, Gentil A (1995) Mutagenicity of a unique 8-oxoguanine in a human Ha-ras sequence in mammalian cells. Carcinogenesis 16:2779–2784

Nakae D, Mizumoto Y, Kobayashi E, Noguchi O, Konishi Y (1995) Improved genomic/nuclear DNA extraction for 8-hydroxydeoxyguanosine analysis of small amounts of rat liver tissue. Cancer Lett 97:233–239

Nakae D, Umemura T, Kurokawa Y (2002) Reactive oxygen and nitrogen oxide species-induced stress, a major intrinsic factor involved in carcinogenic processes and a possible target for cancer prevention. Asian Pac J Cancer Prev 3:313–318

Nishikawa A, Suzuki T, Masumura K, Furukawa F, Miyauchi M, Nakamura H, Son HY, Nohmi T, Hayashi M, Hirose M (2001) Reporter gene transgenic mice as a tool for analyzing the molecular mechanisms underlying experimental carcinogenesis. J Exp Clin Cancer Res 20:111–115

Nishikawa A, Imazawa T, Kuroiwa Y, Kitamura Y, Kanki K, Ishii Y, Umemura T, Hirose M (2005) Induction of colon tumors in C57BL/6J mice fed MeIQx, IQ, or PhIP followed by dextran sulfate sodium treatment. Toxicol Sci 84:243–248

Nohmi T, Suzuki T, Masumura K (2000) Recent advances in the protocols of transgenic mouse mutation assays. Mutat Res 455:191–215

Nohmi T, Masumura K (2005) Molecular nature of intrachromosomal deletions and base substitutions induced by environmental mutagens. Environ Mol Mutagen 45:150–161

Masumura K, Horiguchi M, Nishikawa A, Umemura T, Kanki K, Kanke Y, Nohmi T (2003) Low dose genotoxicity of 2-amino-3,8-dimethylimidazo[4,5-f]quinoxaline(MeIQx) in gpt delta transgenic mice. Mutat Res 541:91–102

Shigenaga MK, Ames BN (1991) Assays for 8-hydroxy-2'-deoxyguanosine: a biomarker of in vivo oxidative DNA damage. Free Radic Biol Med 10:211–216

Takizawa T, Mitsumori K, Takagi H, Onodera H, Yasuhara K, Tamura T, Hirose M (2001) Modifying effects of flumequine on dimethylnitrosamine-induced hepatocarcinogenesis in heterozygous p53 deficient CBA mice. J Toxicol Pathol 14:135–143

Umemura T, Sai-Kato K, Takagi A, Hasegawa R, Kurokawa Y (1996) Oxidative DNA damage and cell proliferation in the livers of B6C3F1 mice exposed to pentachlorophenol in their diet. Fundam Appl Toxicol 30:285–289

Yoshida M, Miyajima K, Shiraki K, Ando J, Kudoh K, Nakae D, Takahashi M, Maekawa A (1999) Hepatotoxicity and consequently increased cell proliferation are associated with flumequine hepatocarcinogenesis in mice. Cancer Lett 141:99–107

Enhanced Spontaneous and Benzo(*a*)pyrene-Induced Mutations in the Lung of Nrf2-Deficient *gpt* Delta Mice

Yasunobu Aoki,[1] Akiko H. Hashimoto,[1] Kimiko Amanuma,[1] Michi Matsumoto,[1] Kyoko Hiyoshi,[1,2] Hirohisa Takano,[1] Ken-ichi Masumura,[4] Ken Itoh,[3] Takehiko Nohmi,[4] and Masayuki Yamamoto[3]

[1]Research Center for Environmental Risk, National Institute for Environmental Studies; [2]Graduate School of Comprehensive Human Sciences; [3]Center for TARA and ERATO-JST, University of Tsukuba, Ibaraki, Japan; and [4]Division of Genetics and Mutagenesis, National Institute of Health Sciences, Tokyo, Japan

Abstract

The lung is an organ that is sensitive to mutations induced by chemicals in ambient air, and transgenic mice harboring guanine phosphoribosyltransferase (*gpt*) gene as a target gene are a well-established model system for assessing genotoxicity *in vivo*. Transcription factor Nrf2 mediates inducible and constitutive expression of cytoprotective enzymes against xenobiotics and mutagens. To address whether Nrf2 is also involved in DNA protection, we generated *nrf2*$^{+/-}$*::gpt* and *nrf2*$^{-/-}$*::gpt* mice. The spontaneous mutation frequency of the *gpt* gene in the lung was approximately three times higher in *nrf2*-null (*nrf2*$^{-/-}$) mice than *nrf2* heterozygous (*nrf2*$^{+/-}$) and wild-type (*nrf2*$^{+/+}$) mice, whereas in the liver, the mutation frequency was higher in *nrf2*$^{-/-}$ and *nrf2*$^{+/-}$ mice than in *nrf2*$^{+/+}$ wild-type mice. By contrast, no difference in mutation frequency was observed in testis among the three genotypes. A single intratracheal instillation of benzo(*a*)pyrene (BaP) increased the lung mutation frequency 3.1- and 6.1-fold in *nrf2*$^{+/-}$ and *nrf2*$^{-/-}$ mice, respectively, compared with BaP-untreated *nrf2*$^{+/-}$ mice, showing that *nrf2*$^{-/-}$ mice are more susceptible to genotoxic carcinogens. Surprisingly, mutation profiles of the *gpt* gene in BaP-treated *nrf2*$^{+/-}$ mice was substantially different from that in BaP-untreated *nrf2*$^{-/-}$ mice. In *nrf2*$^{-/-}$ mice, spontaneous and BaP-induced mutation hotspots were observed at nucleotides 64 and 140 of *gpt*, respectively. These results thus show that Nrf2 aids in the prevention of mutations *in vivo* and suggest that Nrf2 protects genomic DNA against certain types of mutations. [Cancer Res 2007;67(12):5643–8]

Introduction

Nrf2 is an essential transcription factor for inducible and constitutive expression of several phase II detoxification enzymes, including glutathione *S*-transferase-α (GST-α) and GST-π and UDP-glucuronosyl transferase 1A6 (1). Nrf2 also regulates the expression of antioxidant enzymes, including NAD(P)H:quinone oxidoreductase-1 and heme oxygenase-1, in response to oxidative stress (2, 3). Keap1 acts to harness Nrf2 to the cytoplasm, and Nrf2 in this complex rapidly undergoes ubiquitination and proteasomal degradation via Keap1-Cullin 3 E3 interactions (4). However, oxidative or electrophilic modification of Keap1 triggers Nrf2 stabilization (5, 6). During oxidative conditions, Nrf2 translocates into the nucleus and activates cytoprotective gene expression by heterodimerizing with small Maf family members and binding to antioxidant-responsive elements (ARE) or electrophile-responsive element in regulatory regions of cytoprotective genes.

Nrf2-mediated induction of cytoprotective enzymes plays an important role in mitigating the adverse effects of mutagens and oxidants. In Nrf2-deficient mice, which have attenuated basal and inducible expression of these enzymes (7): (*a*) DNA adduct formation is accelerated after diesel exhaust exposure (8); (*b*) hepatotoxicity is enhanced after acetaminophen administration (9); and (*c*) benzo(*a*)pyrene (BaP)–induced DNA adduct and neoplasm formation in forestomach is more prevalent than in wild-type mice (10, 11). Taken together, Nrf2 attenuation or malfunction may be an important aspect of diseases caused by environmental mutagens or oxidants, although the mechanism linking Nrf2 deficiency and mutation frequency is not well understood.

Transgenic guanine phosphoribosyltransferase (*gpt*) delta mice are a model system for detecting *in vivo* mutations (12). In this mouse system, the *gpt* gene is integrated into the genome as a target gene for detecting mutations, and when the *gpt* gene is rescued from genomic DNA to *Escherichia coli*, *gpt* mutants can be randomly selected as rescued *E. coli* colonies that form on plates containing 6-thioguanine (6-TG). To assess whether Nrf2 deficiency increases the mutational risk following exposure to BaP, the current study uses *nrf2*$^{-/-}$*::gpt* mice to analyze mutagenic activity *in vivo*. Furthermore, alterations in the mutation spectrum between *nrf2*$^{+/-}$ and *nrf2*$^{-/-}$ mice were assessed after exposure to BaP.

Materials and Methods

Mice. C57BL/6J *nrf2* knockout mice (7) and *gpt* delta mice (C57BL/6J background; ref. 12) were as described previously, and *gpt* mice were obtained from Japan SLC. Nrf2-deficient mice (*nrf2*$^{-/-}$) were crossed with *gpt* delta transgenic mice (*nrf2*$^{+/+}$*::gpt/gpt*), and the resultant F1 mice (*nrf2*$^{+/-}$*::gpt/0*) were crossed again with Nrf2-deficient mice (*nrf2*$^{-/-}$) to produce *nrf2* knockout *gpt* mice that are homozygous (*nrf2*$^{-/-}$) or heterozygous (*nrf2*$^{+/-}$) to the *nrf2* knockout allele (*nrf2*$^{+/-}$*::gpt* and *nrf2*$^{-/-}$*::gpt*, respectively). Genotyping for *nrf2* was accomplished by PCR amplification of genomic DNA isolated from tails. PCR primers were as follows: 5′-TGGACGGGACTATTGAAGGCTG-3′ (sense for both genotype) and 5′-GCCGCCTTTTCAGTAGATGGAGG-3′ (antisense for wild-type mice) and 5′-GCGGATTGACCGTAATGGGATAGG-3′ (antisense for *LacZ*). The presence of the *gpt* transgene was confirmed by PCR as previously described (12). Nine male Nrf2-deficient *gpt* delta mice (*nrf2*$^{-/-}$*::gpt*) and nine male heterozygous *nrf2* knockout *gpt* delta mice (*nrf2*$^{+/-}$*::gpt*), both 7 to 9 weeks old, were obtained from this breeding scheme. Experiments

---

Note: Supplementary data for this article are available at Cancer Research Online (http://cancerres.aacrjournals.org/).

Y. Aoki and A.H. Hashimoto contributed equally to this work.

Requests for reprints: Yasunobu Aoki, National Institute for Environmental Studies, 16-2 Onogawa, Tsukuba, Ibaraki 305-8506, Japan. Phone: 81-29-850-2390; Fax: 81-29-850-2588; E-mail: ybaoki@nies.go.jp.

doi:10.1158/0008-5472.CAN-06-3355

were done according to protocols approved by the Institutional Animal Care and Use Committee at National Institute for Environmental Studies.

Mouse treatment. BaP (Wako Pure Chemical) was dissolved in tricaprylin $[CH_3(CH_2)_6COOCH_2]_2CHOCO(CH_2)_6CH_3$ (Sigma-Aldrich). Five *nrf2*$^{+/-}$::*gpt* mice and four *nrf2*$^{-/-}$::*gpt* mice were treated with 1 mg BaP dissolved in 50 μL tricaprylin given in a single intratracheal instillation under anesthesia with halothane for mutation analysis as previously reported (13). Vehicle (50 μL tricaprylin) was given to five *nrf2*$^{+/-}$::*gpt* mice and four *nrf2*$^{-/-}$::*gpt* mice as BaP-untreated groups. For immunoblot analysis, three *nrf2*$^{+/-}$ or *nrf2*$^{-/-}$ mice were used for each group. Mice were sacrificed 1 and 14 days after BaP administration under anesthesia with ethyl ether for Western blotting and mutation analysis, respectively. Lungs were removed, quickly frozen in liquid nitrogen, and stored at −80°C until the DNA was isolated.

***gpt* mutation assay.** Genomic DNA was extracted from the lungs using the RecoverEase DNA Isolation kit (Stratagene). Lambda EG10 phages were recovered from the genomic DNA using Transpack Packaging Extract (Stratagene). *E. coli* (YG6020 expressing Cre recombinase) were infected with the recovered phage harboring the *gpt* gene and the chloramphenicol (Cm) acethyltransferase (*cat*) gene (a selection marker), and these genes were rescued as a plasmid (14). The *gpt* mutants can be detected as colonies arising on plates containing Cm and 6-TG. The bacteria were then spread onto M9 salts plates containing Cm and 6-TG, which were incubated for 72 h at 37°C for selection of the colonies harboring a plasmid carrying a mutated *gpt* gene and *cat* gene. The 6-TG–resistant colonies were streaked onto selection plates for confirmation of the resistant phenotype. The cells were then cultured in Luria-Bertani broth containing 25 μg/mL of Cm at 37°C and collected by centrifugation. The bacterial pellets were stored at −80°C until DNA sequencing analysis was done. Mutant frequencies for the *gpt* gene were calculated by dividing the number of colonies growing on (M9 + Cm + 6-TG) agar plates by the number of colonies growing on (M9 + Cm) agar plates, which is the number of colonies harboring the plasmid. To ensure determination of the mutant frequency, mutant colonies were selected from over 300,000 colonies (15).

PCR and DNA sequencing analysis of 6-TG–resistant mutants. A 739-bp DNA fragment containing the *gpt* gene was amplified by PCR using primer 1 and primer 2, as described previously (13). The reaction mixture contained 5 pmol of each primer and 200 mmol/L of each deoxynucleotide triphosphate. PCR amplification was carried out using Ex Taq DNA polymerase (Takara Bio) and done with a Model PTC-100 Thermal Cycler (MJ Research). After the PCR products were purified, sequencing reactions were done by using a DYEnamic ET Terminator kit (Amersham Biosciences). The sequencing primers (primer A and primer C) were as described previously (13).

Immunoblot analysis of GSTs. Frozen lung was homogenized with 2 mL of 50 mmol/L HEPES buffer (pH 7.5) containing 150 mmol/L NaCl, 1 mmol/L DTT, and 0.2 mmol/L phenylmethylsulfonyl fluoride by glass-Teflon homogenizer chilled with ice. The homogenates were subjected to two steps of centrifugation at 4°C (15,000 × *g* for 15 min followed by 100,000 × *g* for 60 min) according to Chanas et al. (16). Resulting 100,000 × *g* supernatants (cytosol fractions) were stored at −80°C until use. After the cytosol fractions mixed with sample buffer containing 1% SDS were heated at 95°C, 9 μg protein (for detecting GST A1/2) or 3 μg protein (for detecting GST A3 and GST P1/2) from each sample was subjected to SDS-PAGE with 15% polyacrylamide gel (17). Proteins separated on the gel were transferred to Immobilon-P membrane (Amersham Biosciences). GST A1/2, GST A3 (18–20), and GST P1/2 were immunochemically detected using anti-mouse GST A1/2 and A3 rabbit sera (kindly provided by Dr. J.D. Hayes, University of Dundee, United Kingdom) and GST P1/2 rabbit serum (kindly provided by Dr. I. Hatayama, Aomori Prefecture Institute of Public Health and Environment, Japan), respectively, and goat anti-rabbit IgG antibody labeled with horseradish peroxidase (16). ECL-plus and Typhoon 9400 BioImage analyzer (Amersham Biosciences) were used to visualize bands.

Statistical analysis. All data are expressed as mean ± SD. Statistical significance of mutant frequency was evaluated using the Student's *t* test. $P < 0.05$ was considered statistically significant. Statistical comparisons of mutational spectra were done using the Adams-Skopek test (21).

Results and Discussion

The frequency of spontaneous mutations in the lung, liver, and testis was compared among *gpt* delta mice (*nrf2*$^{+/+}$), heterozygous mice (*nrf2*$^{+/-}$), and homozygous mice (*nrf2*$^{-/-}$). In the lung and liver, the mutation frequency was significantly elevated in *nrf2*$^{-/-}$ mice, compared with *nrf2*$^{+/+}$ mice (Fig. 1*A*; Supplementary Table S1). The mutant frequency in the lung was approximately three times higher in *nrf2*$^{-/-}$ mice ($1.40 \pm 0.28 \times 10^{-5}$) than *nrf2*$^{+/-}$ and *nrf2*$^{+/+}$ mice ($0.48 \pm 0.05 \times 10^{-5}$ and $0.50 \pm 0.16 \times 10^{-5}$, respectively), whereas the mutant frequency was significantly higher in both *nrf2*$^{-/-}$ and *nrf2*$^{+/-}$ mice ($1.24 \pm 0.13 \times 10^{-5}$ and $1.47 \pm 0.15 \times 10^{-5}$, respectively) than *nrf2*$^{+/+}$ mice in liver ($0.72 \pm 0.24 \times 10^{-5}$). In contrast, no difference in mutation frequency was observed in testis among the three genotypes (Fig. 1*A*). Whereas

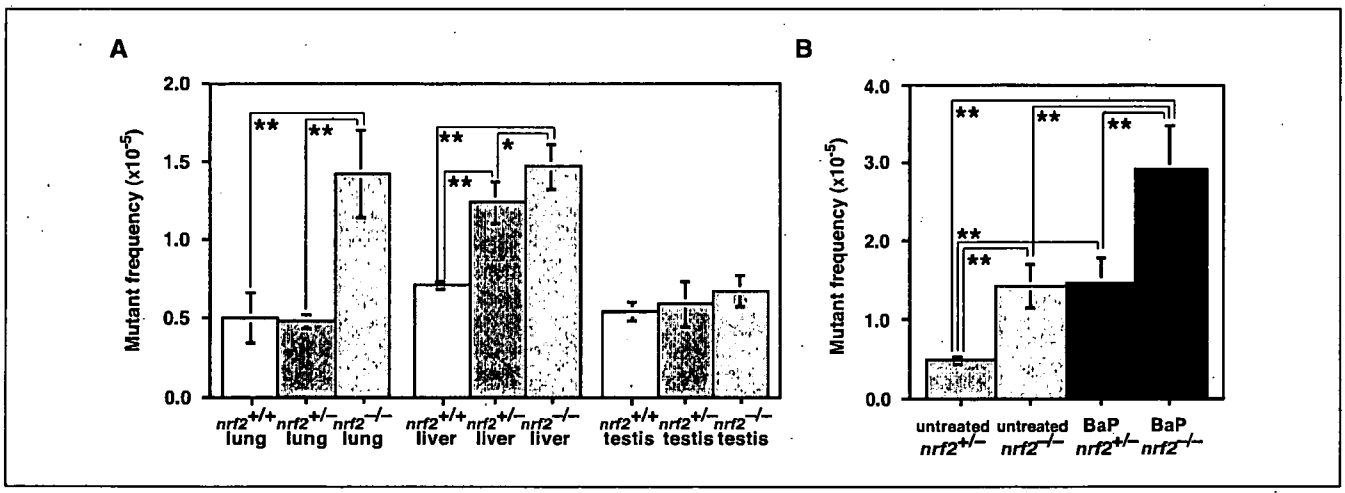

Figure 1. The mutant frequency of 6-TG selection (*A*) in the lung, liver, and testis of *gpt* delta mice (*nrf2*$^{+/+}$, *yellow column*, $n = 3$), and *nrf2*$^{+/-}$ (*light blue column*, $n = 5$) and *nrf2*$^{-/-}$ (*pink column*, $n = 4$) *gpt* delta mice and (*B*) in the lungs of *nrf2*$^{+/-}$ (*blue column*, $n = 5$) and *nrf2*$^{-/-}$ (*red column*, $n = 4$) *gpt* delta mice after BaP treatment. Data of *nrf2*$^{+/-}$ and *nrf2*$^{-/-}$ lungs in (*A*) are replicated as BaP-untreated *nrf2*$^{+/-}$ and *nrf2*$^{-/-}$, respectively, in (*B*). *Columns*, mean; *bars*, SD. *, $P < 0.05$; **, $P < 0.01$, statistical significance among the groups was determined using the Student's *t* test.

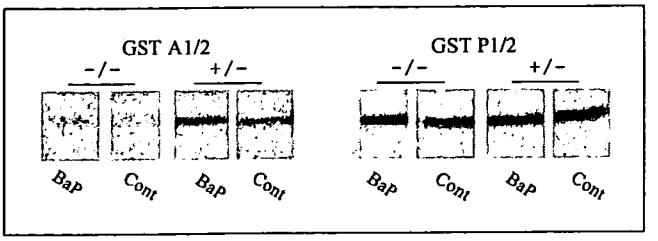

Figure 2. Immunodetection of GSTs. Cytosol fractions were extracted from the lungs of *nrf2*$^{+/-}$ (+/−) and *nrf2*$^{-/-}$ (−/−) mice, separated on SDS/PAGE, and electrophoretically blotted to Immobilon-P membrane. GST A1/2 and GST P1/2 were detected immunochemically using specific antibodies and ECL-plus system. BaP, cytosol fractions extracted from BaP-treated mouse lungs; *Cont*, cytosol fractions extracted from BaP-untreated mouse lungs.

the DNA repair system is quite efficient in the testis (22), metabolically active tissues, such as the liver and lung, seem to be unable to efficiently repair the DNA adducts produced by reactive oxygen species and/or endogenous mutagens without the presence of Nrf2. These results suggest that Nrf2 acts to suppress spontaneous mutagenesis in the lung and liver.

We aimed to quantitatively determine how Nrf2 deficiency affects mutagenicity *in vivo* in the lung using a single intratracheal instillation of BaP as a model environmental mutagen/carcinogen (13). BaP in cigarette smoke or ambient air is readily oxidized to reactive intermediates, such as BaP diol epoxide, by phase I detoxifying enzymes (23), and these intermediates are subsequently metabolized to hydrophilic conjugates by phase II detoxifying enzymes that are under Nrf2 regulation. However, unconjugated reactive intermediates, which often form, lead to DNA adduct formation (24). DNA adducts cause mispairing of DNA bases and induce gene mutations through the DNA replication process (25, 26). This process has been confirmed by *in vitro* experiment using BaP adduct-containing DNA as a template (27, 28). Indeed, a single intratracheal instillation of BaP into *gpt* delta mice resulted in a statistically significant and dose-dependent increase in the mutant frequency in the lungs of *gpt* delta mice, and the most frequent mutation induced by BaP was G:C to T:A transversion (13), which is characteristic of BaP mutagenesis (25, 26).

Therefore, *nrf2*$^{-/-}$*::gpt* and *nrf2*$^{+/-}$*::gpt* mice were given a carcinogenic dose (1 mg; ref. 29) of BaP through trachea, which resulted in a significant increase in the mutation frequency in lungs of both *nrf2*$^{+/-}$ and *nrf2*$^{-/-}$ mice. Importantly, BaP-treated *nrf2*$^{-/-}$ mice had a 2-fold higher mutant frequency ($2.93 \pm 0.56 \times 10^{-5}$) than BaP-treated *nrf2*$^{+/-}$ mice ($1.47 \pm 0.31 \times 10^{-5}$; Fig. 1*B*; Supplementary Table S2). The increment of mutant frequency by BaP treatment was higher in *nrf2*$^{-/-}$ mice than in *nrf2*$^{+/-}$ mice.

We thought that the expression level of Nrf2-regulated cytoprotective enzymes may explain both the higher basal mutant frequency in the Nrf2-deficient mouse and that following treatment of Nrf2-deficient mouse with BaP. Because Chanas et al. have shown that the class π GST isozymes are expressed at substantially lower levels in the livers of Nrf2-deficient mice than in wild-type mice (16). Because a thorough study of pulmonary GSTs in Nrf2-deficient mice has not been described in the literature, we decided to examine whether expression of GSTs was actually suppressed in the lungs of BaP-treated and BaP-untreated *nrf2*$^{-/-}$ mice by immunoblotting. In this study, we have examined expression of GST A1/2, GST A3, and GST P1/2, as these GSTs are known to be under the regulation of the Nrf2-ARE system (7) and are essential for the detoxification of BaP (30). Showing very good agreement with the report by Chanas et al. (16), which analyzed the expression of these enzymes in the mouse livers, the expression level of GST A1/2 was suppressed in the lungs of *nrf2*$^{-/-}$ mice compared with that in the *nrf2*$^{+/-}$ mice (Fig. 2), and the level of GST A3 was also low in Nrf2-deficient mice (data not shown). Under the experimental condition, GST A1/2 level was not elevated substantially by the BaP treatment in the lungs of *nrf2*$^{+/-}$ mice. Similarly, the expression level of GST P1/2 was also suppressed in the lungs of *nrf2*$^{-/-}$ mice compared with that in the *nrf2*$^{+/-}$ mice. GST P1/2 level was elevated by the BaP treatment in the lung of *nrf2*$^{+/-}$ mice, but there was no such difference in *nrf2*$^{-/-}$ mice. As the change in this immunoblotting experiment was relatively small, we repeated this experiment and found that the result was reproducible (data not shown). These results thus suggest that Nrf2 keeps the mutation frequency at low level in the lungs of mice by directing the expression the GSTs. As the changes in this GST immunoblotting experiments was relatively small, we speculate that lack of the

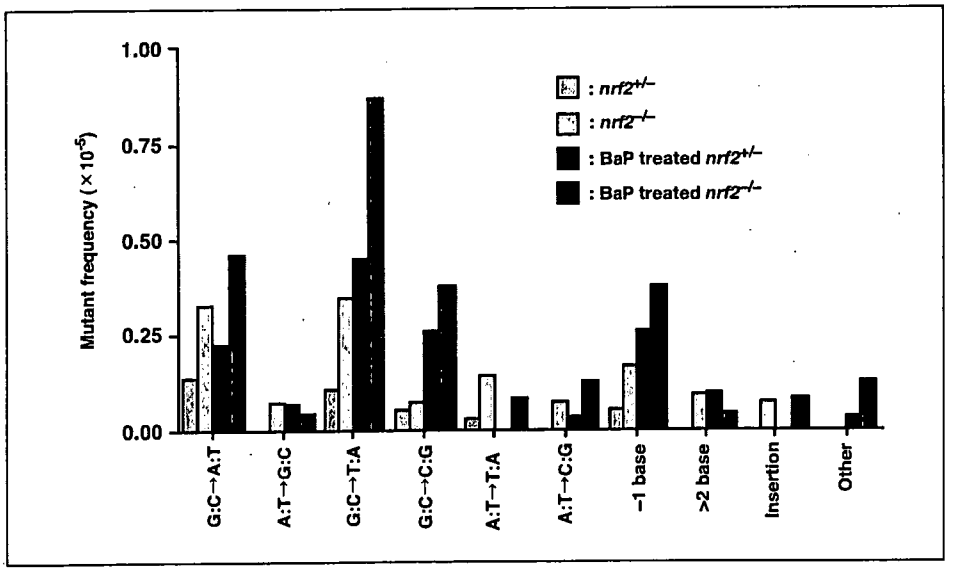

Figure 3. Comparison of mutant frequencies among the types of mutations in BaP-treated and BaP-untreated *nrf2*$^{+/-}$ and *nrf2*$^{-/-}$ mice. *Light blue column*, BaP-untreated *nrf2*$^{+/-}$ mice; *pink column*, BaP-untreated *nrf2*$^{-/-}$ mice; *blue column*, BaP-treated *nrf2*$^{+/-}$ mice; *red column*, BaP-treated *nrf2*$^{-/-}$ mice.

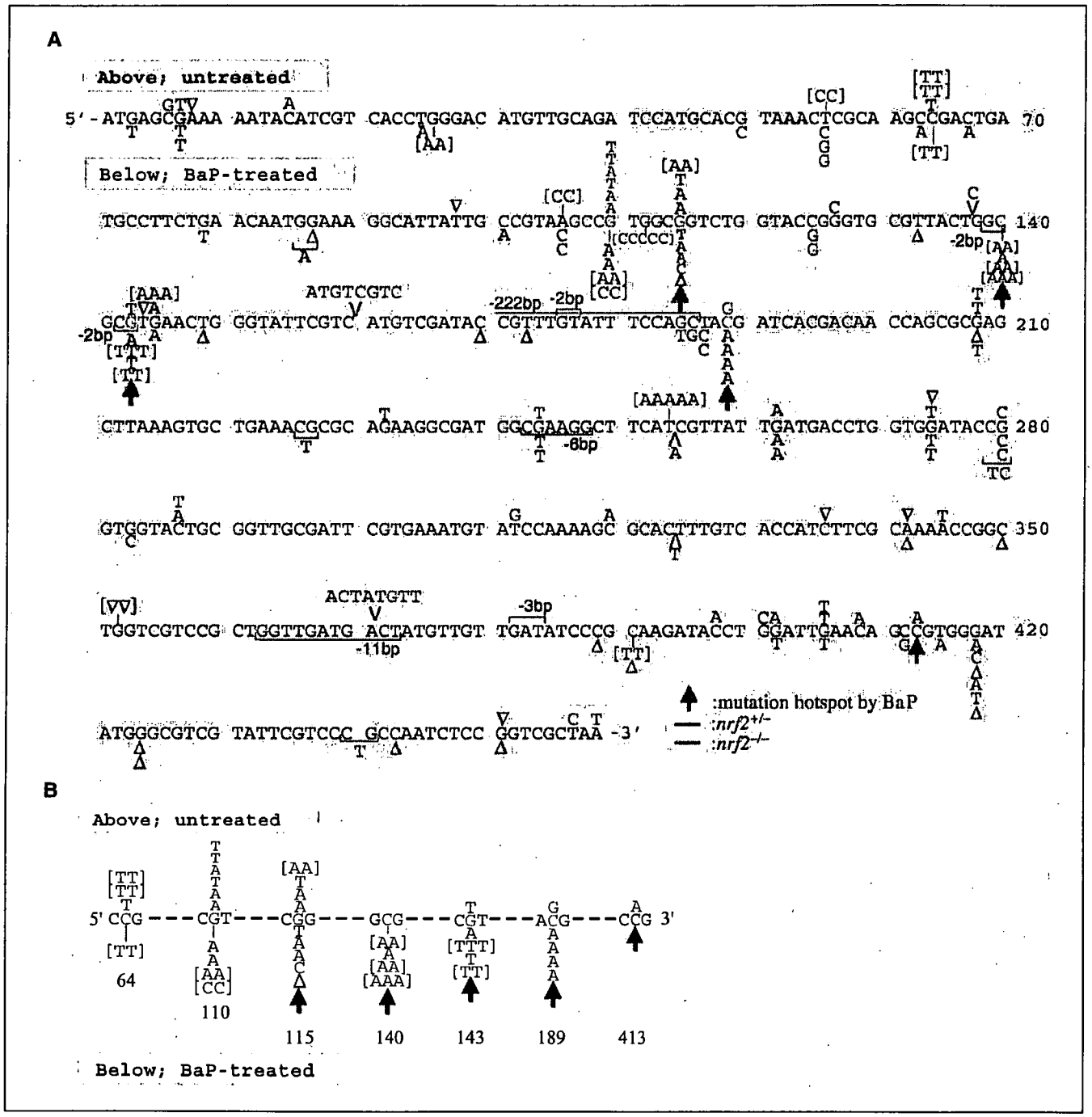

Figure 4. Overall distribution of the mutation detected on the *gpt* gene in the lungs of BaP-treated *nrf2*$^{+/-}$ and *nrf2*$^{-/-}$ mice and BaP-untreated *nrf2*$^{+/-}$ and *nrf2*$^{-/-}$ mice. The mutations are summarized in Supplementary Table S4. *A*, Mutations detected in *nrf2*$^{+/-}$ (*blue*) and *nrf2*$^{-/-}$ (*pink*) mice. The mutations detected in BaP-treated (*below* gpt *sequence*) and BaP-untreated mice (*above* gpt *sequence*). The number of characters in parenthesis is the number of mutations in one mouse. *Δ*, one base deletion; *half-boxes*, deleted nucleotides; *V*, a position of insertion. *Green arrows*, guanine nucleotides of BaP-induced mutation hotspots reported previously (13); *orange characters*, mutation hotspots found in this study. *B*, close-up of hotspots of mutations.

other Nrf2 target genes may also contribute to the mutant frequency in Nrf2-deficient mice.

To further characterize the mutational profile in the lungs of *nrf2*$^{-/-}$*::gpt* and *nrf2*$^{+/-}$*::gpt* mice after BaP exposure, we did DNA sequence analysis of 178 *gpt* mutant lung samples (Fig. 3; Supplementary Table S3). In *nrf2*$^{-/-}$ mice, the predominant spontaneous mutations were G:C to T:A transversion (26%, 15 of 58), G:C to A:T transition (24%, 14 of 58), and base deletions (19%, 11 of 58; Supplementary Table S3). A previous report of *gpt* delta mice (*mmh/ogg1::gpt*) suggested that accumulation of 8-hydroxyguanine in cells was the primary cause of increase in G:C to T:A transversion (31). 8-Hydroxyguanine may also play a role in the

induction of G:C to T:A transversion in the lungs of *nrf2*$^{-/-}$ mice because the level of antioxidant enzymes were suppressed in *nrf2*$^{-/-}$ mice, and subsequently, generation of reactive oxygen spices was probably accelerated.

The BaP treatment increased base substitutions at G:C pairs and one base deletion both in *nrf2*$^{+/-}$ and *nrf2*$^{-/-}$ mice (Fig. 3). Among the G:C substitutions, G:C to T:A and G:C to C:G transversions were markedly elevated in *nrf2*$^{-/-}$ mice after BaP treatment. Consistent with our previous studies with *gpt* delta mice (13), the predominant mutation provoked by BaP treatment was a G:C to T:A transversion (a major base substitute induced by the BaP-DNA adduct formation) in both *nrf2*$^{+/-}$ (32%, 14 of 44) and *nrf2*$^{-/-}$ (34%, 21 of 62) mice (Supplementary Table S2), and the mutant frequency of this transversion was higher in BaP-treated *nrf2*$^{-/-}$ mice than BaP-treated *nrf2*$^{+/-}$ mice (Fig. 3). In the lungs of *nrf2*$^{-/-}$ mice, DNA adducts are probably accumulated in the higher level than those in *nrf2*$^{+/-}$ mice because the expression levels of phase II enzymes that detoxify BaP by forming conjugates (32) and antioxidant enzymes are low in *nrf2*$^{-/-}$ mice comparing to *nrf2*$^{+/-}$ mice. We surmise that this increase of DNA adduct formation might elevate the mutant frequency of G:C to T:A transversion in the Nrf2-deficient condition. Additionally, generation of oxidative DNA adduct due to BaP-derived quinines (33) may be accelerated in *nrf2*$^{-/-}$ mice and play a role, albeit partly, in elevating the mutant frequency in *nrf2*$^{-/-}$ mice. Indeed, BaP adduct formation was accelerated ~2-fold in Nrf2-deficient mouse forestomach compared with wild-type mice (11), supporting our contention that the increase in the amount of DNA adduct enhanced the frequency of these transversions at G:C pairs.

To delineate the mode of mutation in Nrf2-deficient mice, the mutation positions in the *gpt* gene of BaP-treated and BaP-untreated mice were determined (Fig. 4*A*; Supplementary Table S4). Of the mutations found in BaP-treated mice (shown in lower side of the *gpt* sequence; Fig. 4*A*), G:C to T:A transversions at nucleotides 140, 143, and 189 were observed in three or more mice, including both *nrf2*$^{+/-}$ and *nrf2*$^{-/-}$ mice. Thus, these nucleotides are the hotspots of BaP-induced mutation. These nucleotides coincide with those previously reported (i.e., nucleotides 115, 140, 143, 189, and 413; ref. 13), which are shown with green arrows in Fig. 4*A*. The frequency of mutation at these hotspots was rather low in BaP-untreated mice (shown in upper side of the *gpt* sequence; Fig. 4*A*).

Because mutations were accumulated at relatively high level in the *gpt* gene of *nrf2*$^{-/-}$ mice even without BaP treatment, we assumed that we could assess hotspots of spontaneous mutation in these mice. Indeed, G:C to A:T transition at nucleotides 64 was observed in three BaP-untreated mice and one BaP-treated mouse. This mutation is exclusive in *nrf2*$^{-/-}$ mice. Thus, nucleotide 64 is the spontaneous mutation hotspot in Nrf2-deficient condition. In contrast, nucleotides 110 and 115 are common hotspots in BaP-treated and BaP-untreated mice; G:C to A:T transition at position 110 was observed in three BaP-untreated and three BaP-treated mice, and G:C to T:A transversion was also induced in three BaP-untreated mice.

Figure 4*B* shows mutation hotspots in the *gpt* gene. We found that one of the major trinucleotide sequences with BaP-induced guanine nucleotide mutation in this gene was CGT (nucleotides 110, 143, and 189). This is in good agreement with the previous observation that the instillation of BaP into the lung of *gpt* delta mice induced mutations frequently in CGT trinucleotide of the gene (13). CGG (nucleotides 64, 115, and 413) was another frequently found trinucleotide with guanine nucleotide mutations, but no link was found between this mutation and BaP treatment. It should be noted that guanine centered in CGC at position 140 was a frequent target of BaP-induced mutation in Nrf2-deficient condition, whereas previous experiments showed mutations were little in CGC of wild-type mice (13).

Whereas there was no significant difference in the mutation frequency, the position of the mutation was significantly different between BaP-untreated *nrf2*$^{-/-}$ mice and BaP-treated *nrf2*$^{+/-}$ mice (Fig. 4*A*; $P < 0.05$, Adams-Skopek test). This result suggests that chemical mutagenesis and spontaneous mutation in the *nrf2*$^{-/-}$ mice arise through different mechanisms. Thus, the Nrf2 deficiency had a marked affect on the mutational profile that arose either spontaneously or by BaP induction. However, further studies are required to clarify how Nrf2 deficiency alters the mutation profile, and whether nucleotides surrounding the guanine nucleotide are important for the mutation frequency in BaP-treated mice and in BaP-untreated *nrf2*$^{-/-}$ mice.

Several lines of recent evidence have pointed towards a role for Nrf2 in prevention of carcinogenesis. One of the salient examples is that Nrf2 could prevent the formation of DNA adduct and gastric tumors from occurring after BaP administration (10, 11). Furthermore, Nrf2-deficient mice are sensitive to the alkylating agent [*N*-nitrosobutyl(4-hydrixybutyl)amine] and rapidly form bladder tumors after administration (34). This study shows that Nrf2 can prevent increase in the number of spontaneous and inducible mutations that occur in the *gpt* gene in mouse lung and liver and can prevent the induction of mutations at the hotspots, such as nucleotides 64 and 140 in the lung. We surmise that through induction of phase II and antioxidant enzyme activities as well as cross-talk with phase I detoxifying system (35), Nrf2 can mitigate the effects of mutagens, such as BaP, on adduct formation, leading to protection from neoplasm and tumor formation and ultimately aiding in prevention of pulmonary diseases that arise, such as lung cancer from tobacco smoke (36), or from hyperoxic injury (37).

The results presented in this study suggest that Nrf2 deficiency is a possible risk factor for development of lung cancer or other lung diseases caused by mutagens or oxidants in ambient air. Whereas molecular mechanisms by which Nrf2 deficiency changes the mutation profile still require clarification, one plausible explanation is that Nrf2 deficiency may allow accumulation of specific reactive oxygen intermediates or electrophiles. We are now examining how exaggerated mutagenesis in the Nrf2-deficient condition quantitatively contributes to the enhanced carcinogenicity. We believe that the Nrf2-deficient *gpt* delta mice will provide useful information for revealing the relationship between *in vivo* mutagenesis and carcinogenicity.

Acknowledgments

Received 9/18/2006; revised 3/10/2007; accepted 4/9/2007.

Grant support: Japan Society for the Promotion of Sciences grant-in-aid for scientific research 14207100 (Y. Aoki, A.H. Hashimoto, T. Nohmi, and M. Yamamoto) and JST-ERATO (K. Itoh and M. Yamamoto).

The costs of publication of this article were defrayed in part by the payment of page charges. This article must therefore be hereby marked *advertisement* in accordance with 18 U.S.C. Section 1734 solely to indicate this fact.

We thank Dr. John D. Hayes for providing us anti-mouse GST A1/2 and GST A3 antibodies; Dr. Ichiro Hatayama for GST P1/2 antibody; Drs. Hiroaki Shiraishi, Wakae Maruyama, Rie Yanagisawa (National Institute for Environmental Studies), and Jon Maher (University of Tsukuba) for their support and advice; and Yukari Sakashita, Yoshiki Sugawara (National Institute for Environmental Studies), and Katsuyoshi Hayashi (Animal Care Co., Ltd.) for their excellent technical contribution.

References

1. Motohashi H, Yamamoto M. Nrf2-Keap1 defines a physiologically important stress response mechanism. Trends Mol Med 2004;10:549–57.
2. Ishii T, Itoh K, Takahashi S, et al. Transcription factor Nrf2 coordinately regulates a group of oxidative stress-inducible genes in macrophages. J Biol Chem 2000;275: 16023–9.
3. Cho HY, Jedlicka AE, Reddy SP, et al. Role of NRF2 in protection against hyperoxic lung injury in mice. Am J Respir Cell Mol Biol 2002;26:175–82.
4. Tong KI, Kobayashi A, Katsuoka F, Yamamoto M. Two-site substrate recognition model for Keap1-Nrf2 system: a hinge and latch mechanism. Biol Chem 2006; 387:1311–20.
5. Itoh K, Tong KI, Yamamoto M. Molecular mechanism activating Nrf2-Keap1 pathway in regulation of adaptive response to electrophiles. Free Radic Biol Med 2004;36: 1208–13.
6. Kobayashi A, Kang MI, Watai Y, et al. Oxidative and electrophilic stresses activate Nrf2 through inhibition of ubiquitination activity of Keap1. Mol Cell Biol 2006;26: 221–9.
7. Itoh K, Chiba T, Takahashi S, et al. An Nrf2/small Maf heterodimer mediates the induction of phase II detoxifying enzyme genes through antioxidant response elements. Biochem Biophys Res Commun 1997;236: 313–22.
8. Aoki Y, Sato H, Nishimura N, Takahashi S, Itoh K, Yamamoto M. Accelerated DNA adduct formation in the lung of the Nrf2 knockout mouse exposed to diesel exhaust. Toxicol Appl Pharmacol 2001;173:154–60.
9. Enomoto A, Itoh K, Nagayoshi E, et al. High sensitivity of Nrf2 knockout mice to acetaminophen hepatotoxicity associated with decreased expression of ARE-regulated drug metabolizing enzymes and antioxidant genes. Toxicol Sci 2001;59:169–77.
10. Ramos-Gomez M, Kwak MK, Dolan PM, et al. Sensitivity to carcinogenesis is increased and chemoprotective efficacy of enzyme inducers is lost in nrf2 transcription factor-deficient mice. Proc Natl Acad Sci U S A 2001;98:3410–5.
11. Ramos-Gomez M, Dolan PM, Itoh K, Yamamoto M, Kensler TW. Interactive effects of nrf2 genotype and oltipraz on benzo[*a*]pyrene-DNA adducts and tumor yield in mice. Carcinogenesis 2003;24:461–7.
12. Nohmi T, Katoh M, Suzuki H, et al. A new transgenic mouse mutagenesis test system using Spi- and 6-thioguanine selections. Environ Mol Mutagen 1996;28: 465–70.
13. Hashimoto AH, Amanuma K, Hiyoshi K, et al. *In vivo* mutagenesis induced by benzo[*a*]pyrene instilled into the lung of *gpt* delta transgenic mice. Environ Mol Mutagen 2005;45:365–73.
14. Nohmi T, Suzuki T, Masumura K. Recent advances in the protocols of transgenic mouse mutation assays. Mutat Res 2000;455:191–215.
15. Thybund V, Dean S, Nohmi T, et al. *In vivo* transgenic mutation assays. Mutat Res 2003;540:141–51.
16. Chanas SA, Jiang G, McMahon M, et al. Loss of the Nrf2 transcription factor causes a marked reduction in constitutive and inducible expression of the glutathione *S*-transferase *Gsta1, Gsta2, Gstm1, Gstm2, Gstm3* and *Gstm4* genes in the liver of male and female mice. Biochem J 2002;365:405–18.
17. Aoki Y, Satoh K, Sato K, Suzuki KT. Induction of glutathione S-transferase P-form in primary cultured rat liver parenchymal cells by co-planar polychlorinated biphenyl congeners. Biochem J 1992;281:539–43.
18. McLellan LI, Hayes JD. Differential induction of class alpha glutathione *S*-transferases in mouse liver by the anticarcinogenic antioxidant butylated hydroxyanisole. Purification and characterization of glutathione *S*-transferase Ya1Ya1. Biochem J 1989;263:393–402.
19. Hayes JD, Judah DJ, Neal GE, Nguyen T. Molecular cloning and heterologous expression of a cDNA encoding a mouse glutathione *S*-transferase Yc subunit possessing high catalytic activity for aflatoxin B1-8,9-epoxide. Biochem J 1992;285:173–80.
20. Hayes JD, Flangan JU, Jowsey IR. Glutathione transferase. Annu Rev Pharmacol Toxicol 2005;25:51–88.
21. Cariello NF, Piegorsch WW, Adams WT, Skopek TR. Computer program for the analysis of mutational spectra: application to p53 mutations. Carcinogenesis 1994;15:2281–5.
22. Tomascik-Cheeseman LM, Colemana MA, Marchettia F, et al. Differential basal expression of genes associated with stress response, damage control, and DNA repair among mouse tissues. Mutat Res 2004;561:1–14.
23. Buening MK, Wislocki PG, Levin W, et al. Tumorigenicity of the optical enantiomers of the diastereomeric benzo[*a*]pyrene 7,8-diol-9,10-epoxides in newborn mice: exceptional activity of (+)-7beta,8alpha-dihydroxy-9alpha,10alpha-epoxy-7,8,9,10-tetrahydrobenzo[*a*]pyrene. Proc Natl Acad Sci U S A 1978;75:5358–61.
24. Cosman M, de los Santos C, Fiala F, et al. Solution conformation of the major adduct between the carcinogen (+)-anti-benzo[*a*]pyrene diol epoxide and DNA. Proc Natl Acad Sci U S A 1992;89:1914–8.
25. Hakura A, Tsutsui Y, Sonoda J, Tsukidate K, Mikami T, Sagami F. Comparison of the mutational spectra of the *lacZ* transgene in four origins of the Muta Mouse treated with benzo[*a*]pyrene: target organ specificity. Mutat Res 2000;447:239–47.
26. Shane BS, de Boer J, Watson DE, Haseman JK, Glickman BW, Tindall KR. *LacI* mutation spectra following benzo[*a*]pyrene treatment of Big Blue mice. Carcinogenesis 2000;21:715–25.
27. Hanrahan CJ, Bacolod MD, Vyas RR, et al. Sequence specific mutagenesis of the major (+)-anti-benzo[*a*]pyrene diol epoxide-DNA adduct at a mutational hot spot *in vitro* and in *Escherichia coli* cells. Chem Res Toxicol 1997;10:369–77.
28. Chiapperino D, Kroth H, Kramarczuk IH, et al. Preferential misincorporation of purine nucleotides by human DNA polymerase eta opposite benzo[*a*]pyrene 7,8-diol 9,10-epoxide deoxyguanosine adducts. J Biol Chem 2002;277:11765–71.
29. Yoshimoto T, Inoue T, Iizuka H, et al. Differential induction of squamous cell carcinoma and adenocarcinoma on mouse lung by intratracheal instillation of benzo(a)pyrene and charcoal powder. Cancer Res 1980; 40:4301–7.
30. Dreij K, Sundberg K, Johansson AS, et al. Catalytic activities of human alpha class, glutathione transferases toward carcinogenic dibenzo[*a,l*]pyrene diol epoxides. Chem Res Toxicol 2002;15:825–31.
31. Arai T, Kelly VP, Komoro K, Minowa O, Noda T, Nishimura S. Cell proliferation in liver of *mmh/ogg1*-deficient mice enhances mutation frequency because of the presence of 8-hydroxyguanine in DNA. Cancer Res 2003;63:4287–92.
32. Srivastava SK, Watkins SC, Schuetz E, Singh SV. Role of glutathione conjugate efflux in cellular protection against benzo[*a*]pyrene-7,8-diol-9,10-epoxide-induced DNA damage. Mol Carcinog 2002;33:156–62.
33. Burdick AD, Davis JW II, Liu KJ, et al. Benzo[*a*]pyrene quinones increase cell proliferation, generate reactive oxygen species, and transactivate the epidermal growth factor receptor in breast epithelial cells. Cancer Res 2003;63:7825–33.
34. Iida K, Itoh K, Kumagai Y, et al. Nrf2 is essential for the chemopreventive efficacy of oltipraz against urinary bladder carcinogenesis. Cancer Res 2004;64:6424–31.
35. Kohle C, Bock KW. Activation of coupled Ah receptor and Nrf2 gene batteries by dietary phytochemicals in relation to chemoprevention. Biochem Pharmacol 2006; 72:795–805.
36. Wenzlaff AS, Cote ML, Bock CH, Land SJ, Schwartz AG. GSTM1, GSTT1 and GSTP1 polymorphisms, environmental tobacco smoke exposure and risk of lung cancer among never smokers: a population-based study. Carcinogenesis 2005;26:395–401.
37. Cho HY, Jedlicka AE, Reddy SP, Zhang LY, Kensler TW, Kleeberger SR. Linkage analysis of susceptibility to hyperoxia. Nrf2 is a candidate gene. Am J Respir Cell Mol Biol 2002;26:42–51.

Environmental and Molecular Mutagenesis 48:682–693 (2007)

Research Article

Mutations in the Lungs of *gpt* delta Transgenic Mice Following Inhalation of Diesel Exhaust

Akiko H. Hashimoto,[1] Kimiko Amanuma,[1] Kyoko Hiyoshi,[2] Yoshiki Sugawara,[1,3] Sataro Goto,[3] Rie Yanagisawa,[1] Hirohisa Takano,[1] Ken-ichi Masumura,[4] Takehiko Nohmi,[4] and Yasunobu Aoki[1]*

[1]*Research Center for Environmental Risk, National Institute for Environmental Studies, Tsukuba, Ibaraki, Japan*
[2]*Graduate School of Comprehensive Human Sciences, University of Tsukuba, Tsukuba, Ibaraki, Japan*
[3]*Faculty of Pharmaceutical Sciences, Toho University, Funabashi, Chiba, Japan*
[4]*Division of Genetics and Mutagenesis, National Institute of Health Sciences, Setagaya, Tokyo, Japan*

Diesel exhaust (DE) is a major airborne pollutant of urban areas. It contains various polycyclic aromatic hydrocarbons (PAH) and nitrated PAHs. In this study, *gpt* delta mice were treated with inhalation of 1 or 3 mg m^{-3} DE, or a single intratracheal instillation of diesel exhaust particles (DEP) or DEP extract. In the lungs of mice treated with inhalation of 3 mg m^{-3} DE for 12 weeks, the mutant frequency (MF) was 3.2-fold higher than that of the control group (1.90×10^{-5} and 0.59×10^{-5}, respectively). An instillation of DEP and DEP extract resulted in a significant dose-dependent linear increase in MF. In mice treated with 0.5 mg DEP and 0.2 mg DEP extract, the MFs were 3.0- and 2.7-fold higher than that of the control group, respectively. The mutagenic potency (MF mg^{-1}) of DEP extract (5.6×10^{-5}) was double that of DEP (2.7×10^{-5}), suggesting that the mutagenicity of the latter is derived primarily from compounds in the extract, which itself is responsible for ca. 50% of the weight of DEP. G:C→A:T transitions were the predominant *gpt* mutation induced by all three treatments and G:C→T:A transversions were induced by DEP and DEP extract. Guanine bases centered in nucleotide sequences such as GGA, TGA, CGG, and CGT were the major mutation targets of all three treatments. Thus, our results suggest that the mutagens contained in DEP such as PAH and nitrated PAHs induce mutations and may be responsible for carcinogenesis caused by inhalation of DE. Environ. Mol. Mutagen. 48:682–693, 2007.

Key words: diesel emission; diesel exhaust particles; 6-thioguanine selection

INTRODUCTION

Diesel exhaust (DE) is generated by the combustion of light oil and is implicated as a causative agent of lung cancer and allergic respiratory disease, including bronchial asthma [Muranaka et al., 1986]. Diesel exhaust particles (DEP) contain various potent carcinogens and mutagens such as polycyclic aromatic hydrocarbons [PAHs; e.g. benzo[*a*]pyrene (B[*a*]P)] and nitrated PAHs (nitro-PAHs), e.g. 1,6-dinitropyrene (1,6-DNP) [Harris, 1983]. Although some of the compounds in DE have been identified as pulmonary carcinogens in animals [Brightwell et al., 1986], the predominant mutagens remain to be determined.

In rat and mouse lungs, exposure to DEP through inhalation or intratracheal instillation causes oxidative DNA damage [Nagashima et al., 1995; Iwai et al., 2000] and DNA adduct formation [Gallagher et al., 1994; Sato

Abbreviations: B[*a*]P, benzo[*a*]pyrene; DE, diesel exhaust; DEP, diesel exhaust particles; DNP, dinitropyrene; MF, mutant frequency; PAH, polycyclic aromatic hydrocarbons; SPM, suspended particulate matter; 6-TG, 6-thioguanine.

Grant sponsor: Japan Society for the Promotion of Sciences; Grant number:14207100.

*Correspondence to: Yasunobu Aoki, National Institute for Environmental Studies, 16-2 Onogawa, Tsukuba, Ibaraki 305-8506, Japan. E-mail: ybaoki@nies.go.jp

Received 3 December 2006; provisionally accepted 1 July 2007; and in final form 5 July 2007

DOI 10.1002/em.20335

Published online 26 September 2007 in Wiley InterScience (www.interscience.wiley.com).

et al., 2003]. Prolonged inhalation exposure results in respiratory tract tumors in rats [Mauderly et al., 1987; Nikula et al., 1995; Iwai et al., 1997; Valberg et al., 1999]. In rat lung adenomas and adenocarcinomas induced by intratracheal instillation of DEP, point mutations in Codons 12 and 13 of the K-*ras* oncogene have previously been identified [Iwai et al., 1997]. Ichinose et al. [1997] demonstrated the induction of lung tumors in ICR mice treated with 0.05 and 0.1 mg DEP once a week for 10 weeks via intratracheal instillation (30–31%). However, whether or not DE inhalation induces lung tumors in mice remains a matter of debate [Mauderly et al., 1996].

The mutagenicity of DEP extracts has been evaluated in vitro using *Salmonella typhimurium* TA98 assay without an exogenous metabolic activation system (S9 mixture), in which frameshift mutations were found to predominate [Salmeen et al., 1984; Østby et al., 1997; Rivedal et al., 2003]. Although we demonstrated the mutagenicity of DE in vivo using Big Blue® rats [Sato et al., 2000], further studies on its pulmonary effects are required for an assessment of the health risks of air pollution. The present study was undertaken to ascertain the mutant frequency (MF) and spectrum of the mutations induced by inhalation of DE or intratracheal instillation of DEP or DEP extract. To evaluate mutagenicity in vivo, we used *gpt* delta transgenic mice carrying the lambda phage EG10 as a transgene [Nohmi et al., 2000; Thybaud et al., 2003]. When rescued phages are used to infect *E. coli* expressing Cre recombinase, they are converted into plasmids harboring the chloramphenicol (Cm) resistance and guanine phosphoribosyltransferase (*gpt*) genes. *gpt* mutants are selected using plates containing Cm and 6-thioguanine (6-TG).

In this study, inhalation of 3 mg m^{-3} DE (as suspended particulate matter [SPM]) significantly increased MF in a duration-dependent manner. Instillation of DEP (0, 0.125, 0.25, and 0.5 mg) or DEP extract (0, 0.05, 0.1, and 0.2 mg) increased MF in a linear and dose-dependent manner. The mutagenic potency (MF mg^{-1}) of DEP (2.7×10^{-5}) was half of that induced by DEP extract (5.6×10^{-5}). This suggests that the mutagenicity of DEP is derived mainly from compounds in the extract, since ca. 50% of the weight of DEP is provided by the extract. These data suggest that components in the DEP extract were the primary cause of DE-induced mutagenesis in the lungs of mice.

MATERIALS AND METHODS

Treatment of Mice

gpt delta mice carry ca. 80 copies of lambda EG10 DNA on each Chromosome 17 in a C57BL/6J background [Nohmi et al., 1996]. Exposure to DE (12 hr day^{-1}, 7 day $week^{-1}$) was performed in a chamber provided by the National Institute for Environmental Studies [Takano et al., 1998]. A diagram of the chamber can be found in Sagai et al. [1993]. In brief, DE was generated by a computer-controlled light duty (3059 cc) four-cylinder diesel engine (4JG2-type, Isuzu Automobile Company, Tokyo, Japan) run at 1,500 rpm under a load of 10 torques (kg m^{-1}), using standard diesel fuel. The DE generated by this system was injected into a stainless steel dilution tunnel (300 mm diameter × 8,400 mm length), then introduced into the 2.3 m^3 chamber. The residence time of DE in the dilution tunnel was 8.48 sec, and the flow rate in the inhalation zone of the chamber was 0.81 m sec^{-1}. Mice in the control group were maintained in a chamber supplied with filtered clean air. DEP concentration in the chamber was monitored using an Anderson Air Sampler (Shibata Science Technology, Tokyo, Japan); CO concentration was monitored with a CGT-10-3-A portable gas monitor (Shimadzu, Kyoto, Japan). NO and NO_2 concentrations were measured using an NO-NO_2-NO_x analyzer model 43 (Thermo Environmental Instruments, MA). SO_2 concentration was determined by a fluorescent SO_2 analyzer model 8850 (Monitor Labs, CO). The concentrations of DEP (mg m^{-3}), CO (ppm), NO (ppm), NO_2 (ppm), and SO_2 (ppm) were as follows: in the chamber of filtered air, 0.01 ± 0.00 (mean ± SD), 0, 0, 0.15 ± 0.03, and 0.020 ± 0.002, respectively; in 1 mg m^{-3} DE, 0.97 ± 0.16, 10.1 ± 1.5, 11.8 ± 1.5, 4.45 ± 0.64, and 0.204 ± 0.032, respectively; and in 3 mg m^{-3} DE, 2.84 ± 0.47, 25.1 ± 2.0, 26.2 ± 2.4, 9.18 ± 1.83, and 0.320 ± 0.037, respectively. Over 99% (in mass) of DEP was in the 10–470 nm diameter range, and the mass peak was measured at 110 nm diameter using a scanning mobility particle size analyzer (Model 3034, TSI, Tokyo, Japan). The number of DEP particles was estimated as 1.0×10^6 cm^{-3} in 1 mg m^{-3} DE. Three to five, 7-week-old mice were exposed to 1 or 3 mg m^{-3} DE (as SPM) for 4, 12, or 24 weeks. Eleven mice (control group) were maintained in a chamber of filtered clean air. The animals were sacrificed 3 days following the last exposure and their lungs were removed, frozen in liquid nitrogen, and stored at −80°C.

DEP were collected as described previously [Sagai et al., 1993] and the DEP extract was prepared by Dr. Hayakawa [Hayakawa et al., 1997]. In brief, DEP was dispersed in benzene-ethanol (3:1, v/v) and the mixture sonicated. The precipitate was removed by filtration and the supernatant concentrated using a rotary evaporator. The dried concentrate was used as the DEP extract. DEP (0.125, 0.25, or 0.5 mg) or DEP extract (0.05, 0.1, or 0.2 mg) was suspended in 50 μL PBS at pH 7.4 (Gibco BRL, Life Technology, Grand Island, NY) containing 0.05% Tween 80 (Nacalai Tesque, Kyoto, Japan) and 1% DMSO. Each dose was administered to three mice (9-week-old) using a single intratracheal instillation. Each animal was anesthetized with 4% halothane (Hoechst Japan, Tokyo, Japan) until unresponsive to a tactile stimulus. The animal was placed on a restraining board with linen threads to hold the mouth open, and the DEP or DEP extract was instilled into the trachea via a polyethylene tube [Takano et al., 2002; Hashimoto et al., 2005]. As controls, three mice were treated with 50 μL PBS containing 0.05% Tween 80 and 1% DMSO. Mice were sacrificed 14 days after DEP or DEP extract treatment [Suzuki et al., 1999] and their lungs were removed, frozen in liquid nitrogen, and stored at −80°C.

gpt Mutation Assay

The *gpt* assay was performed as described previously [Nohmi et al., 2000]. Genomic DNA was extracted from lung tissue using the Recover-Ease DNA Isolation Kit (Stratagene, La Jolla, CA) and Lambda EG10 phages were rescued using Transpack® Packaging Extract (Stratagene). *E. coli* YG6020 was infected with the phage and spread on M9 salt plates containing Cm and 6-TG [Nohmi et al., 2000], then incubated for 72 hr at 37°C. This enabled selection of colonies harboring a plasmid carrying the gene for chloramphenicol acetyltransferase (CAT), as well as a mutated *gpt*. Isolates exhibiting the 6-TG-resistant phenotype were cultured overnight at 37°C in LB broth containing 25 μg mL^{-1} Cm, then harvested by centrifugation (7,000 rpm, 10 min), and stored at −80°C.

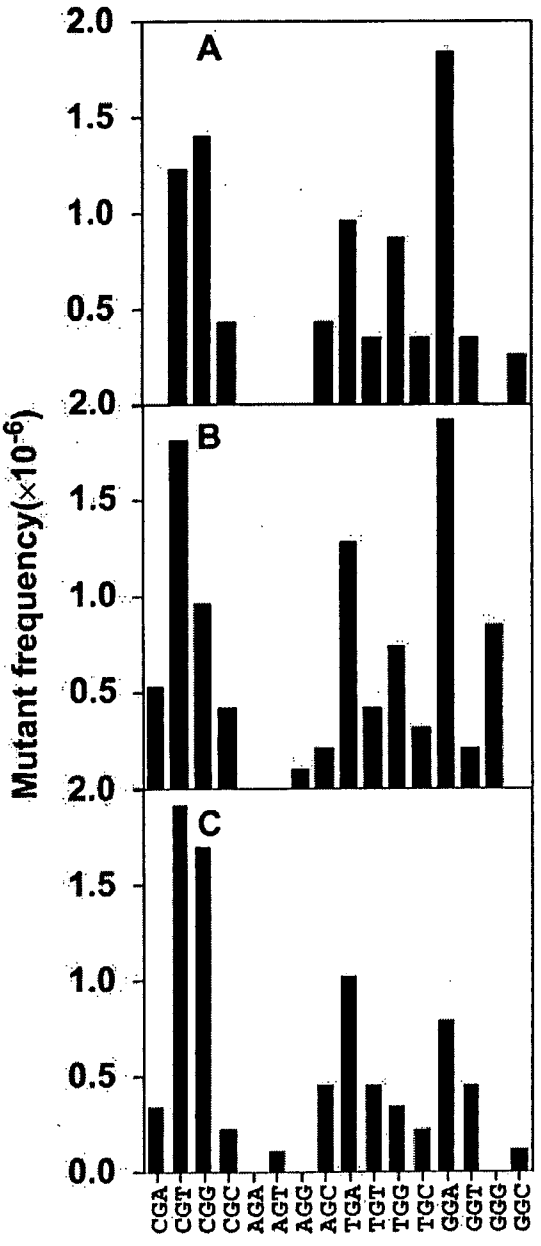

Fig. 1. CG sequence-dependence of *gpt* mutations induced by DE (A), DEP (B), and DEP extract (C).

PCR and DNA Sequencing of the 6TG-Mutants

A 739 bp DNA fragment containing *gpt* was amplified by PCR and sequenced as described previously [Nohmi et al., 2000; Hashimoto et al., 2005]. Sequencing was performed using the Big Dye Terminator v 3.1 Cycle Sequencing Kit (Applied Biosystems, Foster City, CA) on an Applied Biosystems model 3730xl DNA analyzer.

Mutant Frequency

gpt MFs were calculated by dividing the number of colonies growing on (Cm + 6-TG) agar plates by the number growing on Cm agar plates. MFs for each type of mutation in Figure 1 were calculated by dividing the total number of each type of mutant in each group by the total number of colonies growing on Cm agar plates in each group.

Statistical Analyses

All data are expressed as mean ± SD. The statistical significance of DE treatment was analyzed using the Students' t-test; that of the DEP and DEP extract treatments were analyzed using ANOVA with a post-hoc Tukey test. To evaluate the linearity of MF relative to dosage, a simple linear regression was performed. $P < 0.05$ was considered to be statistically significant. Mutational spectra were compared using the Adams–Skopek test [Adams et al., 1987; Cariello et al., 1994].

RESULTS

gpt Mutations in the Lungs of DE-Inhaled *gpt* delta Mice

To estimate the mutagenicity of DE, *gpt* delta mice were exposed to DE (1 or 3 mg m^{-3} as SPM) via inhalation and mutations in the lung were analyzed (Table I). In the lungs of control mice, the background MFs for the 4-, 12-, and 24-week treatment groups were 0.61 ± 0.06 × 10^{-5}, 0.59 ± 0.14 × 10^{-5}, and 0.82 ± 0.07 × 10^{-5}, respectively. In the lungs of the control group, the MF at 24 weeks was a little higher than that at 4 weeks with statistical significance ($P = 0.004$). Although an age-dependent increase in spontaneous MF has been found in the liver, spleen, and adipose tissues of Big Blue® mouse [Hill et al., 2005], MutaMouse [Ono et al., 2004], and *gpt* delta mouse [Masumura et al., 2003], this is the first report of an apparent age-dependent increase in spontaneous MF in the lung. Inhalation of 3 mg m^{-3} DE for 4, 12, and 24 weeks resulted in 1.7-, 3.2-, and 2.6-fold increases in MF (1.06 ± 0.46 × 10^{-5}, 1.90 ± 0.88 × 10^{-5}, and 2.11 ± 0.08 × 10^{-5}, respectively) compared with the control mice during the same time period (Table I). Thus, the MF reached a plateau after 12 weeks of DE inhalation. Significant increases in MF were observed between groups treated with 3 mg m^{-3} DE via inhalation for 12 or 24 weeks, compared with the 4-week group (Table I). A 3.1-fold (1.84 ± 0.82 × 10^{-5} vs. 0.59 ± 0.14 × 10^{-5}) increase in MF was observed between mice treated for 12 weeks with 1 mg m^{-3} DE via inhalation and control mice; however, there did not appear to be a significant difference between the MF at 1 mg m^{-3} as compared to 3 mg m^{-3} DE.

Mutations Caused by Instillation of DEP and DEP Extract

Mice were treated with a single intratracheal instillation of DEP or DEP extract. Instillation of 0.125, 0.25, and 0.5 mg DEP increased the MF by 1.8-, 2.1-, and 3.0-fold (1.16 ± 0.01 × 10^{-5}, 1.40 ± 0.05 × 10^{-5}, and 1.97 ± 0.18 × 10^{-5}, respectively), compared with control mice (0.66 ± 0.08 × 10^{-5}) (Table II). Instillation of 0.05, 0.1, and 0.2 mg DEP extract increased the MF by 1.5-, 1.9-, and 2.7-fold (0.97 ± 0.10 × 10^{-5}, 1.28 ± 0.11 × 10^{-5}, and

TABLE I. Summary of Mutant Frequency in the Lungs of *gpt* delta Mice After Inhalation of DE

DE concentration (mg m^{-3})	Exposure time (weeks)	ID of animals	Number of colonies		Mutant frequency (10^{-5})	Average mutant frequency ± SD (10^{-5})
			Mutant	Total		
Control	4	1	4	763,100	0.52	0.61 ± 0.06
		2	6	964,500	0.62	
		3	5	758,300	0.66	
		4	6	920,400	0.65	
		Total	21	3,406,300		
3	4	1	17	1,735,400	0.98	1.06 ± 0.46[a]*
		2	16	1,002,200	1.60	
		3	15	1,019,500	1.47	
		4	9	1,405,000	0.64	
		5	9	1,449,000	0.62	
		Total	66	6,611,100		
Control	12	1	3	377,600	0.79	0.59 ± 0.14
		2	2	360,500	0.55	
		3	4	852,000	0.47	
		4	2	360,000	0.56	
		Total	11	1,950,100		
1	12	1	9	309,600	2.91	1.84 ± 0.82[a]*
		2	9	448,000	2.01	
		3	9	859,200	1.05	
		4	4	289,600	1.38	
		Total	31	1,906,400		
3	12	1	15	537,600	2.79	1.90 ± 0.88[a]*[c]*
		2	10	438,400	2.28	
		3	8	932,000	0.86	
		4	7	654,400	1.07	
		5	12	476,800	2.52	
		Total	52	3,039,200		
Control	24	1	13	1,551,000	0.84	0.82 ± 0.07[b]*
		2	8	1,074,000	0.74	
		3	8	903,000	0.89	
		Total	29	3,528,000		
3	24	1	10	462,500	2.16	2.11 ± 0.08[a]***[c]**
		2	11	546,000	2.01	
		3	16	745,600	2.15	
		Total	37	1,754,100		

Statistical significance was determined using a Students' t-test.
[a]Significant differences between the control and DE-treated groups.
[b]Significant difference to the control group at 4 weeks.
[c]Significant differences compared with exposure to 3 mg m^{-3} DE via inhalation for 4 weeks.
*$P < 0.05$; **$P < 0.01$; ***$P < 0.001$.

$1.78 \pm 0.19 \times 10^{-5}$, respectively), compared with control mice. The MF increased linearly for 0–0.5 mg DEP ($r^2 = 0.95$; $P < 0.001$ [Table II]) and 0–0.2 mg DEP extract ($r^2 = 0.94$; $P < 0.001$), suggesting that DEP extract as well as DEP has a potential to induce mutations in the lung.

Mutation Spectrum Induced by DE Inhalation

To determine the mutation spectrum induced by DE inhalation, we sequenced 126 and 55 *gpt* mutants from the lungs of treated and control mice, respectively. The types of mutation were analyzed and the mutations in treated and control mice are presented in Table III. In groups that inhaled DE, 55% (69/126 mutants) of the mutations were G:C → A:T transitions and 17% (21/126) were G:C → T:A transversions, whereas in control mice, 40% (22/55 mutants) of mutations were G:C → A:T transitions and 31% (17/55) were G:C → T:A transversions. In the DE-treated mice, the percentage of G:C → A:T transitions was increased and the percentage of G:C → T:A transversions was decreased by prolonged inhalation of DE for 24 weeks, whereas in the control mice the mutation types remained constant. At 24 weeks, the Adams–Skopek test showed a significant difference ($P = 0.04$) in mutation spectrum between the control and DE inhalation group; G:C → A:T transitions were elevated from 44 to 77% and G:C → T:A transversions were reduced from 28 to 8% by DE inhalation. The frequency of spontaneous